Simulation of R.F window Brazing process: Thermal-Structural analysis of ceramic to metal vacuum brazing joints

A Thesis Submitted in Partial Fulfilment of the Requirements for the Degree of

Master of Technology (Research)

in

Mechanical Engineering

By

Sandeep Kumar Singh
Roll No: 610ME803

Under The Guidance of
Prof R. K. Sahoo
Shri Anjan Dutta Gupta

Department of Mechanical Engineering
National Institute of Technology
Rourkela 769008, India

2013

NATIONAL INSTITUTE OF TECHNOLOGY

ROURKELA—769008
INDIA

Anjan Dutta Gupta
SO/G
VECC, DAE, Kolkata

R. K. Sahoo
Professor
NIT Rourkela

CERTIFICATE

This is to certify that the thesis entitled "Simulation of R.F window brazing process: Thermal-Structural analysis of ceramic to metal vacuum brazing joints", being submitted by Shri Sandeep Kumar singh, is a record of bona fide research carried out by him at Mechanical Engineering Department, National Institute of Technology, Rourkela and Variable Energy Cyclotron Centre, Kolkata, under our guidance and supervision. The work incorporated in this thesis has not been, to the best of our knowledge, submitted to any other university or institute for the award of any degree or diploma.

(Anjan Dutta Gupta) **(R. K. Sahoo)**

Date: Mar , 2013

Dedicated to

My Family members

&

My all well wishers

Acknowledgement

I would like to extend my sincere gratitude and respect to my supervisors Prof. R.K Sahoo and Shri Anjan Dutta Gupta for their excellent guidance, suggestions, constructive criticism, encouragement and support. Their knowledge and perseverance has always been a motivation for working harder and towards achieving higher goals. I am thankful to them for their time and the effort which they dedicated, which helps a lot to complete this thesis and for the overall development of my career. I feel proud that I am one their Master's students. The charming personality of Prof. R .K. Sahoo has been combined perfectly with knowledge that creates a permanent impression in my mind. I also feel lucky to get Shri Anjan Dutta Gupta Head, MEDRD VECC and as one of my supervisor for his help in modeling and simulation. His invaluable academic and creative suggestions helped me a lot to complete the project successfully. His liberal attitude encouraged me to have a friendly interaction, which never made me feel the burden of work.

I record my appreciation for the help extended by Prof. R.K. Sahoo during my research work. I am thankful to Mr. Trijit Kr. Maiti, Mr. Subrata saha, Mr. Manir ahmmed, Mr. K majumdar, Mr. T.K Debnath, Mr. Tapas Mallik, Mr. D Adak, Mr. S.C Sarkar Mr. K Virachary & all officers , staffs of Mechanical Engineering group , Mr. Amitava Sur (Ex-HOD Vacuum section),Dr. N.K das, Mr. Sudhir mondal, Mr. R.C Yadav & Mr. S Bhattacharya of Vacuum section, Mr. S. Som Head, R.F division Variable Energy Cyclotron Centre, Kolkata for sharing their vast experience on design and machining , providing ready made parts and inspection of very tight tolerance components.

I indebted my gratitude to, EX- Director of CGCRI Prof. H.S Maiti, present Director of CGCRI Prof. Indranil Manna, Mrs. Sumana Ghosh (Das) and Dr. Someswar Dutta, Division Head Bioceramics and Coating division CSIR-CGCRI Kolkata, Mr. Nandadulal Dandapat from BESU Kolkata, for their permission to execute the job , expertise advise, supports time to time for experimental work.

I am obliged to present Director NIT Rourkela Dr. Sunil Kr. Sarangi EX-Director VECC Dr. R.K Bhandari, present Director, VECC Dr. D.K Srivastava , Associate Director Dr. Alok Chakraborty, Ex- Head- MEG Shri Jayanta Chaudhuri,

and present Head- MEG Shri Gautam Pal, Head-CPIEG,VECC Shri R Dey , for allowing me to continue and complete my research work .

I take this opportunity to express my heartfelt gratitude to all the staff members of Mechanical Engineering Department, NIT Rourkela, CGCRI and VECC, Kolkata for their valuable suggestions and timely support. Lastly, but not the least I would like to thank all my friends of NIT, Rourkela and colleagues of VECC, Kolkata who helped me directly or indirectly throughout the course of this work.

I would like to thank the faculty member of NIT Rourkela Dr. Alok Sathpathi, Dr. Ashok Sathpathi, Prof. R.K Sahoo my friends H. Barke, Mr. T Rakesh Krishnan, Mr. Srimant Mishra, Mr Balaji kumar chowdhury, Mr. Binay kumar from NIT Rourkela for their valuable discussions.

I would like to thank my family for their support and motivation throughout the course of this dissertation. Last but not the least I would like to thank the Almighty God.

March: , 2013 **Sandeep Kumar Singh**

Abstract

The creation of the cyclotron absolutely sited radio frequency at the centre of particle accelerators. In the cyclotron, RF system is a device that transforms electrical energy taken from the grid into energy transferred to a beam of particles inside the accelerating cavity. The power coupler, which transport and inject power to the cavity, needs at the same time to couple strongly the transmission line to the field distribution in the cavity. It also has to provide a way to adjust the matching between the line and the cavity, and finally to separate the vacuum of the cavity from the air of the line. The consequence of these multiple requirements is that the power coupler is usually a very critical device that requires a careful design and prototyping. R.F window is one of the main parts of the power coupling capacitor.

The present research work dealt with the simulation of R.F window brazing process & development of ceramic to metal (copper) outer joint of R.F window. The outer brazing joint is very critical as higher thermal expansion material, e.g. copper is placed outside of the lower linear thermal expansion coefficient material (ceramic). It results a large brazing gap – not suitable for capillary action. A detailed analysis was performed from simple model to FEM model (using theoretical approach & FEM code, Ansys.) to understand the behavior during brazing. Molybdenum & Graphite both had been considered separately as tooling fixture material for theoretical and FEM analysis. Literature review reported that maximum work in the field of ceramic to metal brazing have been adopted using molybdenum as tooling fixture. In this research work Graphite was selected as tooling fixture material to perform the vacuum brazing process of ceramic to copper outer joint test model. After design and dimensions, model drawings were developed. Fabrication of the test model assembly, brazed inside vacuum brazing furnace by using Cusil filler. This joint has qualified Helium leak test in order of 3.6×10^{-9} mbar l/s.

Contents

Nomenclature

κ	=	Thermal diffusivity	(m^2/s)
T	=	Temperature	(Centigrade or Kelvin)
r	=	radius	(mm)
i	=	subscript	
ε	=	emissivity	
σ	=	Stefan and Boltzman constant	($W/m^2\ K^4$)
σ_r	=	Radial stress	(N/m^2) or MPa.
σ_θ	=	Hoop or tangential stress	(N/m^2) or MPa.
MSLD	=	Mass Spectrometer Leak Detector	
ε_r	=	Strain in radial direction	
ε_θ	=	Strain in angular direction	
ε_z	=	Strain in axial direction	
C1, C2	=	Constant	
α	=	Coefficient of linear expansion	μm/m K
ν	=	poisson ratio	
ΔT	=	Difference in temperature	^{0}C or K
p	=	pressure	(N/m^2) or MPa.
a,b	=	Surface identification	
u_r	=	deformation in radial direction	(mm)
u_θ	=	deformation in angular direction	(mm)
u_z	=	deformation in axial direction	(mm)
SS	=	Stainless steel	
T_o	=	Standard temperature	(273 K)
t	=	Time	(sec)
δ_b	=	Interface displacement	(mm)
t_{min}	=	Minimum wall thickness	(mm)
k_1,k_2,k_3,k_4	=	Geometrical ratio constant	
Cu	=	Copper (OFHC)	
Mo.	=	Molybdenum	
Al.	=	alumina	

p_b	=	Interface pressure	(N/m2 or MPa.)
S.P	=	Set point	
P.V	=	Process value	
E	=	Modules of Elasticity	(N/m2 or GPa.)
R.F	=	Radio frequency	
REF.	=	Reference	
BKIN	=	Bilinear kinematics	
Se	=	secant constant	
L	=	length	(mm)
RP	=	Reference point	
RM	=	Modified reference point	
Sx	=	radial stress	(N/m2 or MPa.)
Sy	=	hoop stress for plane stress model	(N/m2 or MPa.)
Sz	=	hoop stress for axisymmetric model	(N/m2 or MPa.)
SEQ	=	Vonmises stress	(N/m2 or MPa.)
FEM	=	Finite element method	

List of Figures

Page No.

Chapter 1

Chapter 3

Chapter 4

Chapter 5

List of Tables

Page No.

Chapter 3

Appendix

Chapter 1

INTRODUCTION

1.1 Background

For several decades, cyclotrons were the best source of high-energy beams for nuclear physics experiments. A cyclotron is a type of particle accelerator, it accelerate charged particles to increase their kinetic energy. These high-energy particles are also used, e.g. in nuclear research or in hospitals to obtain radioactive preparations for medical and diagnostic purposes. K-500 Super conducting cyclotron is an advanced creation of conventional cyclotron (R.T), which is designed to feed 100 kV R.F voltage for accelerating charged particle rotating in high magnetic field. Super conducting coil immersed in liquid helium bath at 4K is main component to produce high magnetic field. The room temperature R.F system generates high electric field between the Dee-gap of beam space. R.F system consists of cavities, amplifier, transmission line and coupling capacitor. Coupling capacitor couples the cavities and power amplifier through R.F transmission line. The R.F window and surrounding assemblies , which provides path for R.F power in-to accelerating structure coupling circuit is called coupling capacitor. The purpose of R.F windows is to provide vacuum barrier while feeding R.F power to the cavities. This research work is allied for R.F window brazing simulation by using ANSYS code prior to fabrication commenced. A block diagram of R.F power transmission and a general arrangement showing key components has been illustrated in Fig. 1.1 & Fig. 1.2.

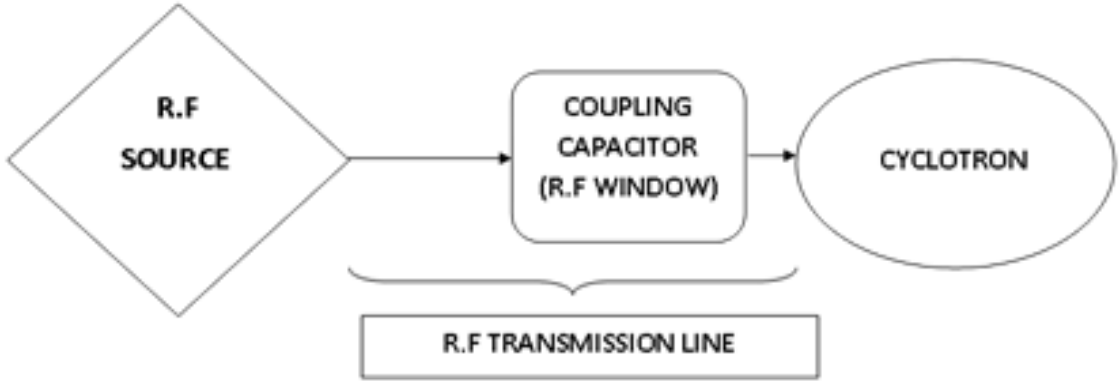

Fig.1.1: Block diagram of R.F power feeding from R.F source to cyclotron

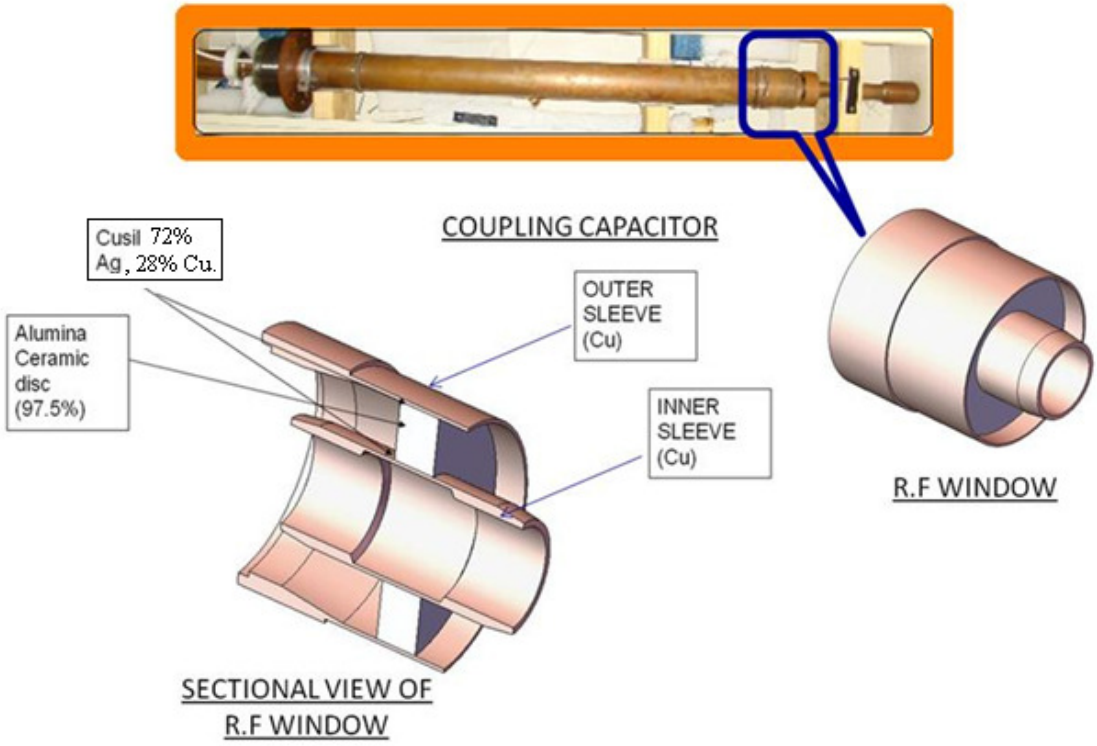

Fig.1.2: General arrangement of R.F window & coupling capacitor

1.2 Need of a R.F window

R.F window is a vacuum brazed (alumina to copper) assembly and it is one of the main parts of coupling capacitor of K-500 Super conducting cyclotron. It is a critical component for the input coupler in any particle accelerator, especially in recent accelerator development involving continuous wave and superconducting application. During feeding of micro wave power, it also acts as a vacuum barrier. The failure mechanism of RF window is mostly due to multipacting, the bombardment of electrons on the ceramic window surface, which leads to thermal heating and eventually failure of the windows.

The continuous operation of cyclotron requires standby coupling capacitor to reduce the down time of cyclotron operation. In-house fabrication of coupling capacitor needs RF window as a spare. A comprehensive study and simulation analysis of ceramic to metal brazing inside vacuum furnace is required a prior to the fabrication of R.F window.

1.3 Basic principle of ceramic to metal vacuum brazing joint

The basic principle of metal to ceramic brazing in the vacuum furnace brazing process consists of heating the piece parts, braze materials, and guide rings of fixture, followed by the subsequent flow of the braze material and thereafter, cooling of the brazed assembly and fixture.

This theory is relevant in the manufacturing of R.F window; wherein thin ceramic disc is brazed to copper sleeves using a brazing furnace. The result is a RF window that provides a vacuum barrier between the copper sleeves and the environment and allows passage of RF power over a certain frequency bandwidth. The alumina ceramic has a much lower thermal coefficient of expansion than the copper sleeve or braze material. Guide ring is used to control the radial gap between the copper sleeve and ceramic window during the furnace brazing operation. The guide ring is usually molybdenum, which has a thermal coefficient of expansion close to the ceramic. Due to the mismatch between the thermal expansion coefficient of ceramic and copper sleeve, large internal stresses develop as the finished assembly cools after the braze joint is made. These stresses could become large enough to produce micro-cracks in the braze joints itself and also in ceramic around braze joint area.

In addition, the combination of high tensile residual stresses around the brazed joint and operating stress applied can promote brittle fracture and increase the susceptibility of a brazed joint during service. Being able to quantify these residual stresses is a key step in determining the continuing integrity of the RF window. Hence it is important to estimate the residual stresses in brazed joint to assure the integrity of the structure. However, pure experimental approaches will cost a lot for this small-scale and complex RF window structure. Therefore, finite element modeling becomes a relevant tool to predict the brazing temperature and residual stress. With the development of computer technology, finite element method has been used to predict brazing temperature and residual stress successfully. In this work, a sequentially thermal and structural coupling residual stress analysis procedure has been developed to study the characteristics of brazing temperature field and residual stress after completion of brazing process for alumina ceramic to copper inner and outer conductor of RF window structure. Block diagram showing simple model has been illustrated in Fig. 1.2.

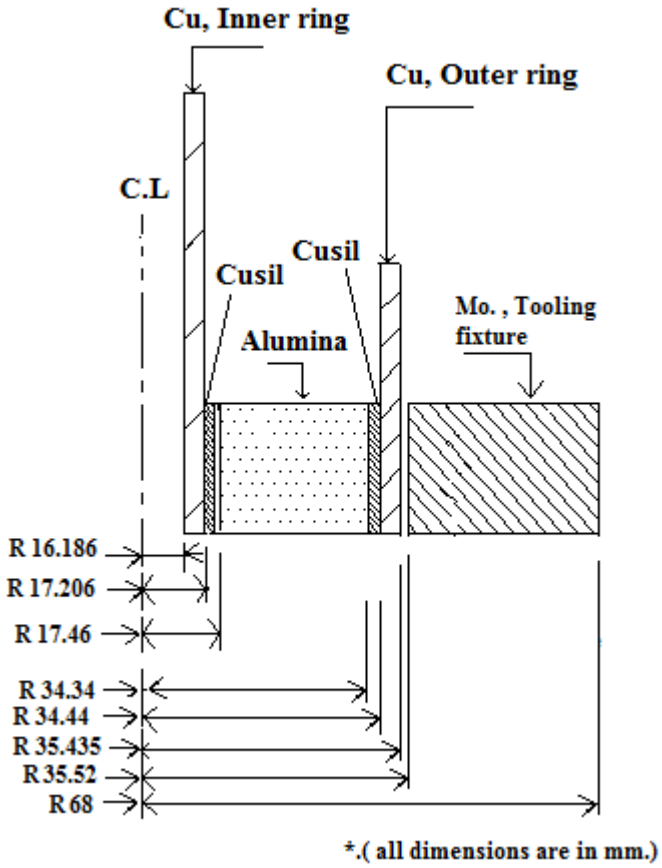

Fig.1.3: Simplified block diagram of model

At present almost all the premier technological research and educational institutes, Atomic Energy Establishment, Space Research Center, etc are widely using electrical feed through for various research works. Therefore, study of ceramic to metal brazed feed through assembly becomes an essential device for all those users.

1.4 General specification of prototype R.F window for simulation analysis and development

In R.F window a ceramic disk is brazed, between two copper co-axial sleeves, to form a vacuum-tight RF window. Inner and outer sleeve materials are OFHC 99.95% copper and insulator material, Alumina 97.5%. A guide ring is used to restrain the thermal expansion of the copper sleeve to control the braze gap. This introduces radial and hoop compression in the copper sleeve and ceramic during the heating phase, which must be accounted for as initial conditions to the cooling phase. Molybdenum 99.95% pure has been selected as fixture material, due to its low thermal expansion coefficient, close to the ceramic and has good thermal conductivity

1.5 Objectives of the project

At present we import coupling capacitor which is not only very expensive in terms of foreign exchange but also a time consuming process. And also we are to depend on foreign nations for its spares. This project primarily aims at developing this device indigenously and to study short term and long term performance of system. The objectives of this work are outlined as follows:

i. Simulation of RF window brazing process: Thermal-structural design analysis of the assembly

ii. Systematic procedure for development of ceramic to metal braze joint

iii. Performance study of R.F window with various test setups for helium leak test, R.F high voltage testing, joints destructive testing.

iv. In house development of various components of R.F window at VECC workshop and NIT Rourkela in collaboration with private manufacturers. The components include metalized ceramic, molybdenum or graphite fixture, OFHC copper inner and outer conductor, eutectic copper silver filler foil etc.

v. Proper documentation for future construction on commercial basis and technology transfer.

1.6 Organization of the thesis

This thesis has been set in six chapters.

Chapter 1 deals with a general introduction to R.F window and its uses in various cyclotron fields for research and development. It also defines the scope of the work.

Chapter 2 presents a brief review of the literature, covering the experimental techniques of using different types of model joining technique and analysis with various FEM code e.g. ANSYS, abacus etc. The literature review also provides the information regarding the current research and the performance of the R. F window already installed in several cyclotrons or particle accelerators centers throughout the globe.

Chapter 3 illustrates the basic ceramic to metal joining principles and several joining theories. R.F window outer joint is studied at first because of its different materials required to be joined having different thermal expansion coefficient. The lower thermal coefficient material is inside and higher one is at outside of assembly. This chapter describes the clearance between the materials to be joined and the tooling fixture.

Chapter 4 describes the details of fabrication, pre-cleaning, brazing procedure, and post cleaning.

Chapter5 reveals the evaluation and quality control of brazed joint theory and the methodology applied to test the joint leakage using helium leak detection method by MSLD.

Chapter6 describes the summary and conclusions for the present status and future scope of the work. In this chapter the aim at the time of starting and target achieved have been described.

The bibliography and supporting documents are enlisted at the end of the manuscript.

Chapter 2

LITERATURE REVIEW

2. Literature review

[1] In this manual different type of metal to ceramic joints development described, beginning from material selection, metallization, cleaning of parts after machining, brazing, test of joints etc. Metals to ceramic seals have been in existence for thousands of year since early man first made decorative objects. Little progress was made in nineteenth century with the innovation of internal combustion engine required a spark plug. Since then , there have been considerable technological advancement, particularly in electron tube industry for this type of joints. FARRELL L DEIBEL [2] has simulated the thermal structural analysis of entire furnace brazing process of R.F window for getting the residual manufacturing stresses in the brazing joint. He has described the complete brazing cycle analysis of ceramic disc, brazed into copper sleeve to form a vacuum tight R.F window. For this simulation of the brazing cycle finite –element ANSYS code has been used. He defined, the basic theory of complete heating and cooling brazing cycle of R.F window fabrication in ANSYS code by deriving an equation i.e. secant linear coefficient of expansion based on braze temperature as reference. He also suggested that simulation of both the heating and cooling phases must be performed in complete close cycle, as the guide ring does restrain the copper sleeve during RF window assembly furnace brazing process. His analysis focused on deriving new methodology to keep one temperature reference point for simulating the model because at present, ANSYS does not have a provision for the multiple TREF's that exist in the cooling phase. The approach in ANSYS to solving this problem involves a restart to link the heating and cooling phases; however, a complication arises in the calculation of thermal strain within the computer code.

R.A RIMMER [3] discussed the design, fabrication and testing of a high power alumina disc window in WR 1500 wave guide at L Band, suitable for use in the NLC damping ring RF cavities at 714 MHz and LEDA accelerator at 700MHz. His assembly design follows the procedure development of PEP-II. He has used molybdenum as keeper ring to provide proper brazing gap at braze temperature. He has defined the brazing

furnace temperature set point with rate of heating and the process was simulated in ANSYS to fine tune the dimension and several ring test were checked without ceramics first to check the parameter. Finally by some minor modification in process subsequent braze were successful. MICHAEL NEUBAUR [4] has well established the design of RF window by studying of ceramic material characterization, compression ring design, modeling the brazing process & effect of pre-stressed in disk window. His designed ensured the capability of R.F window to bear the tensile stress generated by R.F heating by placing ceramic window into compressed state. Compression ring is made of stainless material which is coated by copper to ensure proper braze joint. He has provided molybdenum keeper ring to maintain the braze gap at brazing temperature.

Data obtained from available various research works , some basic idea has been adopted in present work that metals expand when they are heated, and contract when they are cooled. This phenomenon has been thoroughly explored over the years, and data-tables have been published showing how fast each metal expands as temperature increases. This important information about the expansion characteristics of each metal should always be used in developing braze procedures when different kinds of base metals are to be brazed to each other. The success or failure of a braze procedure may very well depend on it.

The optimal braze joint clearance that is needed for a successful braze occurs AT BRAZING TEMPERATURE, since only at brazing temperature is the brazing filler metal (BFM) liquid and therefore able to flow through the joint by capillary action. Thus, it is critical that to use the metal expansion data from the charts to "back-calculate" from the needed clearance at brazing temperature down to the room temperature clearance needed to give us that desired clearance at brazing temperature when the two metals are heated (for most brazing we typically want a 0.002-0.005" {0.050-0.125mm} clearance between the joining surfaces. If the I.D. of the low thermal expansion coefficient material (say alumina) exactly matched the O.D. of the round high thermal expansion coefficient material (say copper). What will happen as that assembly is heated to brazing temperature? The copper expands faster than the alumina, the clearance (braze-gap) between the two parts will shrink (get tighter) as the temperature increases. In fact, the joint may become so tight that no BFM would be able to penetrate through it. Similarly, in case of copper as the outer cylinder and the alumina as a smoothly fitting insert into the copper sleeve, we can see that the gap clearance between the two surfaces would get

wider with increasing temperature. The effect of thermal expansion must be taken into account ahead of time before the parts are made, so that the metal parts may be appropriately machined before they are assembled for brazing in order to achieve optimal clearance at brazing temperature to let capillary energy do its work.[15,16]

Several researchers have worked for design analysis and finally fabricated a various type of R.F window as per the requirement by developing a dissimilar metal vacuum brazing joining process. But none has addressed more design analysis of co-axial type RF window. Hence, the present study aims at investigating the design analysis of co-axial R.F window braze joint structure in order to enhance the database of thermal and structural stress analysis and to gain sufficient knowledge by using 2D axisymmetry FEA model ANSYS code and their solutions to encourage greater and effective application of the knowledge. The present research work involves simulation of brazing cycle by using molybdenum and graphite as tooling fixture. Finally graphite has been selected as tooling fixture for vacuum brazing of R.F window outer joint development test setup .

2.1 History of development

In [14] it is described that metal to ceramic joining has been an area , which is under continuous development process for last few decades due to its massive scope in various field like the aerospace industry, electronic tube industry, biomedical implant industry etc. Depending upon the application and the base metal to be bonded various techniques are utilized for metal-to ceramic joints. Ceramic and metals can be joined brazing, diffusion bonding etc. Joining ceramic to metal by brazing technique is utilized where joints might get exposed to temperature as high as 500^{o}C. Structural ceramics as, SiC, Al2O3 and others have been successfully brazed to a number of metals and alloys.

2.1.1 Brazing fundamental

Brazing is a joining technique need not require any melting or plastic state of the base metal. In this process coalescence is produced by heating to a temperature higher than 450 ^{o}C (If the liquidus is below 450 ^{o}C, the process is called soldering) and by using a filler metal that should have a liquidus temperature higher than 450 ^{o}C and below the solidus temperature of the base metal. The filler metal is filled between the closely fitted surfaces of the joint by capillary action. Brazing has four different characteristics:

- The coalescence, or joining, is achieved by heating the assembly or the region of the parts to be joined to a temperature of 450 ^{o}C or above.
- Assembled parts and filler metals are heated up to a temperature to melt the filler metal but not the parts.
- The molten filler metal filled into the joint and wet the base metal surfaces.
- The parts are cooled to solidify the molten filler metal, which is held in the joint by capillary action and holds the part together.

2.1.2 Adhesion, Wetting, Spreading and Capillary action

The adhesion wetting , spreading and capillary action driving force is surface tension between solid liquid and vapor. The Young's equation for non-reactive liquid on an ideal solid (physically and chemically inert, smooth, homogeneous and rigid) states that, with a decrease in the contact angle the liquid drop surface area increases and hence the total liquid surface free energy increases. The driving force for wetting is difference between the surface tension of solid vapor and solid liquid is more than the surface tension between liquid vapor.

2.1.3 Challenges in Joining Ceramics

Ceramics are poorly wetted by brazing alloys. This poor wettability is causing due ionic ad covalent bonding in their lattice due to which the electron movement is restricted. There are two methods to overcome the poor wetting characteristic of ceramic materials. Metallization of ceramic and active metal brazing are such types of methodology.

In the first approach a surface treatment is provided on to the ceramic surface to decrease the surface energy and to alter the interfacial thermodynamics to provide a better wettable surface to braze metal/alloys, this is known as metallization of ceramics. There are several ways to metalize the ceramics as follows.

- Coating of Mo-Mn process followed by sintering
- Co-fired Ni electroplating, W and and Ag-Cu braze
- Mechanical metallization
- Thin film deposition over ceramic by Physical vapor deposition (PVD),[14]

2.1.4 Other challenges in vacuum brazing of alumina ceramic to metals

In the earlier section it has been discussed that joining ceramic to metal is not a simple process and one of the reason being the poor wettability of ceramic by filler metals used n brazing. Another challenge that has to overcome to join ceramic to metal is the difference in the coefficient of thermal expansion between metal and ceramic surfaces. When the brazed joint is cooled down from the brazing temperature to the room temperature there are significant stress developed at the joint. One way to minimize or release the residual stresses is the use of a ductile filler metal or use of a ductile metal interlayer that undergoes plastic deformation to improve these stresses and keep the brazed joint sound and leak proof. In the present work Cusil is used as braze filler metal which is very ductile and its uses reduced the residual stress build up at the joint.[32]

Chapter 3

DESIGN, SIMULATION & DRAWING DEVELOPMENT OF CERAMIC TO METAL BRAZING JOINTS MODEL

This chapter presents the design calculation and drawing development of all major mechanical components of R.F window. The model consists of OFHC inner and outer conductor, alumina ceramic coated by Mo-Mn and Ni plated at inner and outer surfaces. Molybdenum and graphite are selected as tooling fixture material for analysis. The design methodology of the ceramic to metal brazing of R.F window consists of the following units, which are illustrated in the subsequent sections.

- Analytical simulation, for deformation of Alumina ceramic & copper.
- Analytical & FEM simulation of deformation and stress analysis for compound cylinders in plane stress model
- FEM simulation for three cylinder axisymmetry model heating cycle by generating contact and target elements.
- FEM - simulation for RF window axisymmetry model using Molybdenum tooling fixture for heating and cooling cycle by generating contact and target elements (non-linear).
- FEM-simulation for Fabrication trial of outer brazing joint model using graphite tooling fixture.
- Drawing development

3.1 Analytical simulation, for deformation of Alumina ceramic and copper:

Since R.F main components is alumina ceramic and OFHC copper sleeve. Alumina ceramic is required to join with copper sleeve at inside and outside its periphery. These joints have to be vacuum tight joint in-order $1X10^{-9}$ torr, L / sec. The criticality of joints is its different coefficient of thermal expansion material to be joined by vacuum brazing process. Brazing process required 0.05 mm to 0.1 mm gap between parts to be joined. This stringent requirement is due to providing capillary action at brazing temperature for filling the gap by molten filler material. In this research work outer joint has been analysed to keep the necessary gap between ceramic and copper. Analysis of joint clearance has been done as follows:

3.1.1 Physical dimension & Elastic properties of alumina disc

$r_{Al300(inside)}$ = 17.46 mm, $r_{Al300(outside)}$ = 34.34 mm,

α_{Al300} = 7.89 X 10^{-6} m/m K, (average) [Data from Annexure]

3.1.2 Physical dimension & Elastic properties of OFHC copper

$r_{cu(inside)}$ = 34.34 mm to 34.44 mm, $r_{cu(outside)} = r_{cu(in)}$ + 1.02 mm,

α_{cu} = 19.13 X 10^{-6} m/m K, (average) [Data from Annexure]

3.1.3 Temperature of joining

- Room Temperature = 300 K
- Brazing Temperature = 1100 K (Using value of Cusil filler liquidus temperature = 780^0 C)

3.1.4 Model governing equation:

Consider a one dimension case of thin disc subjected to the temperature T is constant . It is assumed further that stress and displacements also do not vary over thickness. Body force is ignored. Also because of symmetry, $\tau_{r\theta} = 0$ and with $\sigma_z = 0$ as thin disk assumed . This is plane stress case and deformation in radial direction can be given as follows:

$$u_r = r\alpha\Delta T \qquad (3.1.1)$$

$$\delta = u_r^{cu} - u_r^{ceramic} \qquad (3.1.2)$$

$u_r^{cu} = r_i^{cu} . \alpha^{cu} . \Delta T$ (3.1.2a)

$u_r^{ceramic} = r_o^{ceramic} . A^{ceramic} . \Delta T$ (3.1.2b)

where, u_r = deformation due to change in temperature,

r_i = dimension at room temperature (i= Cu, ceramic (Al300.))

α_i = Average Coefficient of thermal expansion

ΔT = Difference in temperature

δ = Clearance at brazing temperature

u_r^{cu} = Deformation of copper inner dia.

$u_r^{ceramic}$ = Deformation of ceramic Alumina 300 outer dia.

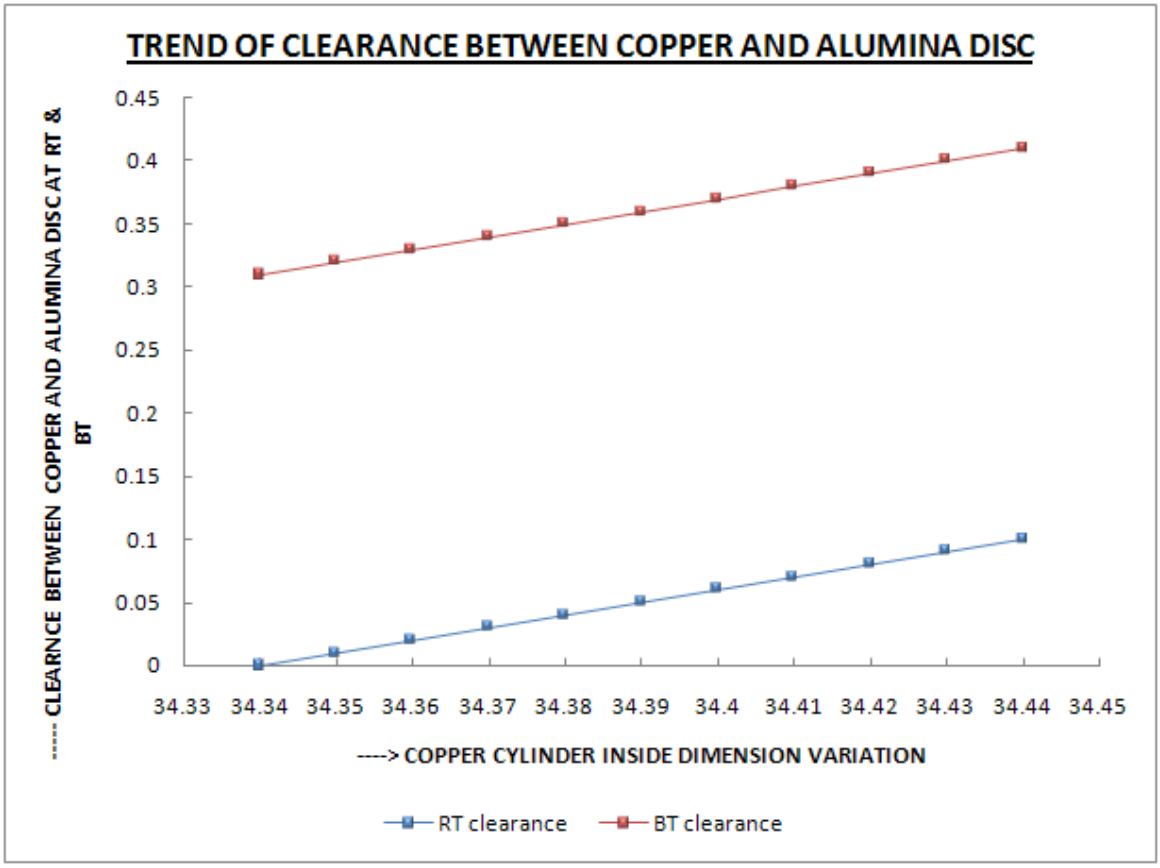

Fig.3.1: Trend of Clearance between copper and Alumina disc without tooling fixture

3.1.5 Results and discussion :

Solution of Equation (3.1.1) & (3.1.2) provides result of clearance trend , plotted in fig. 2. From above plotted results it shows that the clearance value (zero) at room temperature increases up to 0.300 mm. This gap is too large for capillary action, required for brazing & it increases with increasing room temperature clearance. So this analysis states that for appropriate gap at brazing temperature some tooling fixture is needed, which prevent the control the expansion of copper, so that proper gap at brazing temperature can be achieved. This tooling fixture must have low coefficient of thermal expansion, good thermal conductivity and elastic property up to brazing temperature. Molybdenum and graphite properties are suitable for the tooling fixture. In this research both materials have been analysed as tooling fixture and finally easily available pyrolitic graphite has been used for trail test of vacuum brazing process. Next step is finding plane stress value in two cylinder when comes in contact after heating by analytical and FEM simulation.

3.2 Analytical & FEM simulation of deformation and stress analysis for compound cylinder in plane stress model :

In this section a details analytical and FEM simulation (ANSYS code) method used. The desired brazing gap and stress value between copper and ceramic obtained by providing a tooling fixture . The gap in range of 0.05 mm to 0.150 mm is required for filling the braze gap by capillary action. Tooling fixture check the deformation of copper to maintain the desired gap. In this analysis a simple one dimension model is analysed to get the desired dimension of tooling fixture and copper sleeve. The methodology adopted is as follows :

3.2.1 Analytical simulation

3.2.1.1 Model governing equation:

Consider a compound thick cylinder with open end shown as follows. It is loaded by contact pressure p_b. The contact pressure arises due to difference in thermal expansion coefficient. Higher thermal expansion coefficient material is kept inside of lower thermal coefficient material. The stresses that arise when copper is heated to the brazing temperature are proportional to the difference in thermal expansion of guide ring (Molybdenum/graphite) and the outer conductor(Copper). Deformation due to both free thermal expansion and thermal stress are defined after some assumptions are as follow .

Assumptions: We shall assume that $\sigma_z = 0$ (axial stress). Owing to uniform radial deformation , neglecting body force and uniform body temperature. End of cylinders are free to expand. This case is plane stress case.

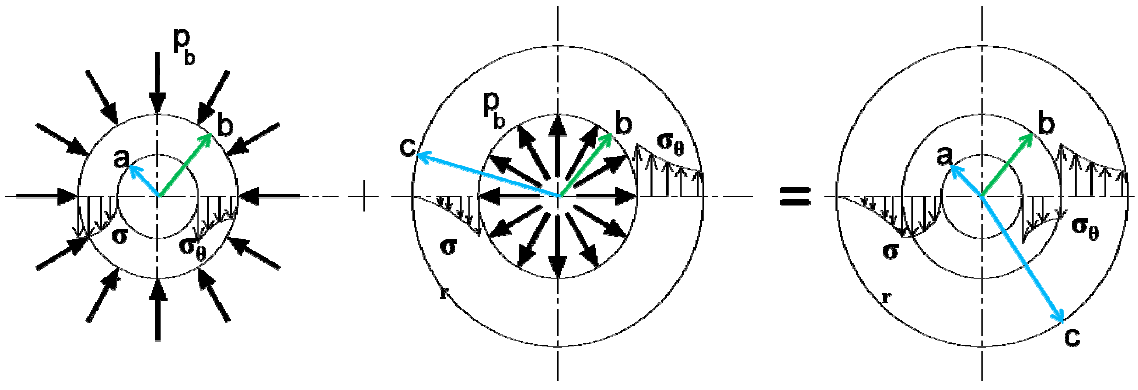

Fig.3.2: Schematic diagram of compound cylinder under thermal stress

Due to internal & external pressure zero, the interface pressure can be calculated by using Lame's equation as followings (Details in Annexure 2):

$$p_b = \frac{\Delta T.(\alpha_1 - \alpha_2)}{\frac{k_3 + \nu_2}{E_2} + \frac{k_2 - \nu_1}{E_1}}, \tag{3.2.1}$$

3.2.1.2 Radial & Hoop stress for Cylinder under external pressure

$$\sigma_{r(Cu.)} = \frac{-b^2.p_b}{b^2 - a^2} + \frac{p_b.a^2.b^2}{b^2 - a^2}.\frac{1}{r_{Cu.}{}^2} \tag{3.2.2}$$

$$\sigma_{\theta(Cu.)} = \frac{-b^2.p_b}{b^2 - a^2} - \frac{p_b.a^2.b^2}{b^2 - a^2}.\frac{1}{r_{Cu.}{}^2} \tag{3.2.3}$$

3.2.1.3 General displacement equation for Cylinder under internal & external pressure

$$u_{r(Cu.)} = \frac{1}{E_1.(b^2 - a^2)}\left[(1-\nu_1).\left(a^2.p_a - b^2.p_b\right)r_{Cu.} + (1+\nu_1).a^2.b^2\left(p_a - p_b\right).\frac{1}{r_{Cu.}}\right] \tag{3.2.4}$$

3.2.1.4 Radial & Hoop stress for Cylinder under internal pressure

$$\sigma_{r(Mo.)} = \frac{-b^2.p_b}{c^2 - b^2} - \frac{p_b.a^2.b^2}{c^2 - b^2}.\frac{1}{r_{Mo.}{}^2} \tag{3.2.5}$$

$$\sigma_{\theta(Mo.)} = \frac{-b^2.p_b}{c^2 - b^2} + \frac{p_b.a^2.b^2}{c^2 - b^2}.\frac{1}{r_{Mo.}{}^2} \tag{3.2.6}$$

3.2.1.5 General displacement equation for Cylinder under internal & external pressure

$$u_{r(Mo.)} = \frac{1}{E_2.(c^2 - b^2)}\left[(1-\nu_2).\left(b^2.p_b - c^2.p_c\right)r_{Mo.} + (1+\nu_2).b^2.c^2\left(p_b - p_c\right).\frac{1}{r_{Mo.}}\right] \tag{3.2.7}$$

3.2.1.6 Results of Thermal Stress Analysis by analytical method:

In the present analysis at the time of heating copper and tooling fixture material will come in contact after some time of heating from 300K to 758.139K. Room temperature dimension and Average elastic properties of copper cylinder (r_i^{cu} = 34.36 mm, r_o^{cu} = 35.38 mm α^{cu}= 19.13 x 10^{-6} m/m K, ν^{cu}=0.36) and Molybdenum (r_i^{Mo} = 35.602 mm, r_o^{Mo} = 68 mm, α^{Mo}= 5.4 x 10^{-6} m/m K, ν^{Mo}=0.31). Alumina ceramic ($r_i^{ceramic}$ = 17.46 mm, $r_o^{ceramic}$ = 34.34 mm, $\alpha^{ceramic}$= 7.89 x 10^{-6} m/m K, $\nu^{ceramic}$=0.32).Here copper having high thermal expansion coefficient placed inside of tooling fixture material Molybdenum having low thermal expansion coefficient placed at outside. Temperature of contact has been calculated as follows:

$$\delta = r_i^{Mo} - r_o^{Cu} \text{ (Clearance at RT)} \quad (3.28)$$

$$= u_{ri}^{Cu} - u_{roi}^{Mo} \text{ (Difference in deformation at BT)} \quad (3.29)$$

The above equations provide the difference in room temperature to contact temperature

$$\Delta T_{contact} = \frac{\left(r_i^{Mo} - r_o^{Cu}\right)}{\left(\left(r_o^{Cu}.\alpha^{Cu}\right) - \left(r_i^{Mo}.\alpha^{Mo}\right)\right)} \text{ (DetailsAnnexure-1)} \quad (3.30)$$

Then, the contact temperature $T = 300 + \Delta T_{contact}$ (3.31)

Equation (3.31) gives the average temperature at the time of contact is 758.19 K .Heating of assembly from temperature at the time of contact to brazing temperature (1100 K), there will be a contact pressure (p_b) developed at the point of contact. Due to this contact pressure thermal tensile stress in molybdenum cylinder and compressive thermal stress develop in copper cylinder will be produced.

From eq. (3.2.1), after assuming pressure in-side (p_a) and out-side ($p_{c)}$ of cylinder is zero. The contact pressure p_b = 15.886 N/m^2 will acts for copper cylinder as cylinder under external pressure and for molybdenum cylinder as cylinder under internal pressure. From eq. 3.2.2 to eq. 3.2.7 maximum and minimum radial and hoop stress in copper and molybdenum are as follows:

STRESS AND DEFORMATION VALUE				
Type of stress	**Material**	**Inside cylinder**		**Outside cylinder**
Radial stress (N/m^2)	Copper	0		-15.886
	Molybdenum	-15.886		0
Hoop stress (N/m^2)	Copper	-559.085		-543.199
	Molybdenum	27.884		11.998
Clearance between copper and ceramic	Material with dimension	Copper I.D (mm)	Ceramic O.D (mm)	Clearance (mm)
	Room temperature dimension	34.36	34.34	0.02
	Brazing temperature dimension	34.671	34.557	0.114

Table 3.1: Analytical result of stress and deformation

The result shown in table 1 that stress values are crossing the yield limit of copper, so copper will get deformed during cooling and the final dimension will be less than RT

dimension. Ceramic will not allow deforming more so a compressive stress will be developed at joint, which will further enhance the integrity for the joint. The gap between copper and ceramic at brazing temperature is 0.114 mm. This is much less than without tooling fixture and also within range as per brazing standard. This result is further verified by FEA simulation of two compound cylinder PLANE STRESS case.

3.2.2 FEA simulation using Ansys code:

There is various simulation code developed for general purpose finite element analysis. Ansys is using for this research work. It is founded in 1970 by Dr. John A Swanson. It provides powerful simulation software and technologies to suit of engineering simulation tools which accelerates the product development process at less computational and financial expenditure.

3.2.2.1 Ansys Analysis (Plane stress and axisymmetry results of model up-to brazing temperature or heating cycle):

a) PLANE STRESS MODEL :

Plane stress is a state of stress in which normal stress σ_z and shear stresses τ_{xz} and τ_{yz} directed perpendicular to the normal stress are assumed to be zero. In the present research work the ends of cylinder are free to expand. According to Hooke's law stresses σ_r (radial stress) and σ_θ (hoop stress) produces a uniform extension or contraction in z direction, and cross-sections perpendicular to the axis of cylinder remain plane. If we consider two adjacent cross-sections, the deformation undergone by the element does not interfere with the deformation of the neighboring element. Here, the elements can be considered to be in a state of plane stress.

In present analysis there is two cylinder of different coefficient of thermal expansion placed coaxially and heated uniformly. The higher coefficient of thermal expansion material is exerting pressure (placed inside) on outside cylinder (lower thermal expansion coefficient) after some time. This contact pressure acts for both cylinder as internal and external cylinder under pressure.

Consider a co-axial cylinder shown in fig. 3.3 a 2D structural solid element PLANE 55 (Thermal analysis) followed by PLANE 42 (Structural analysis) is used to perform the analysis. One material model is defined. Solid modeling approach is employed. Geometric entity model is shown in fig 3.4. Maximum deflection, maximum

radial and hoop stress induced in the cylinder are determined. Material properties are defined in annexure.1. Let the assumption are as followings:

- 2 D Plane stress Linear analysis
- Uniform heating
- Open end long cylinder

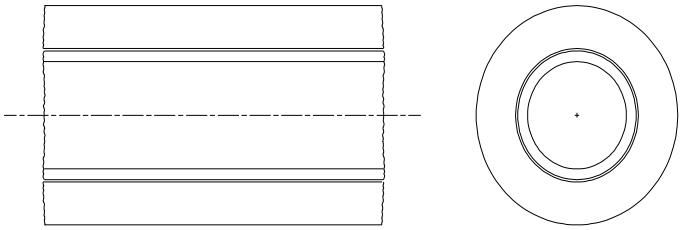

Fig.3.3: Long cylinder compound pressure vessel

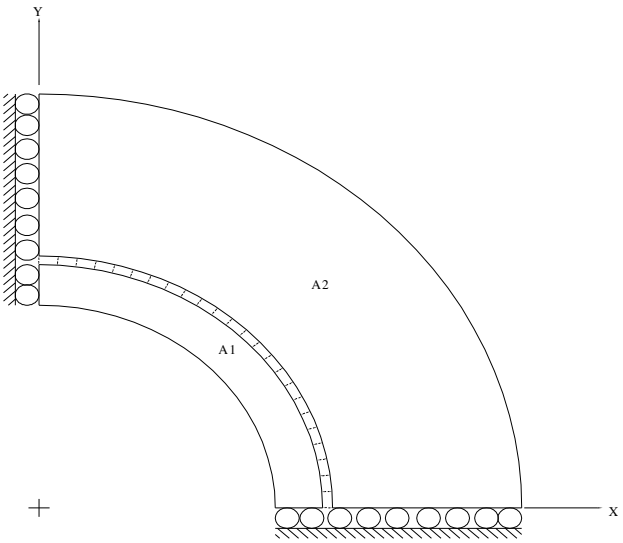

Fig.3.4: Geometric entity of plane stress model

Results & discussion :

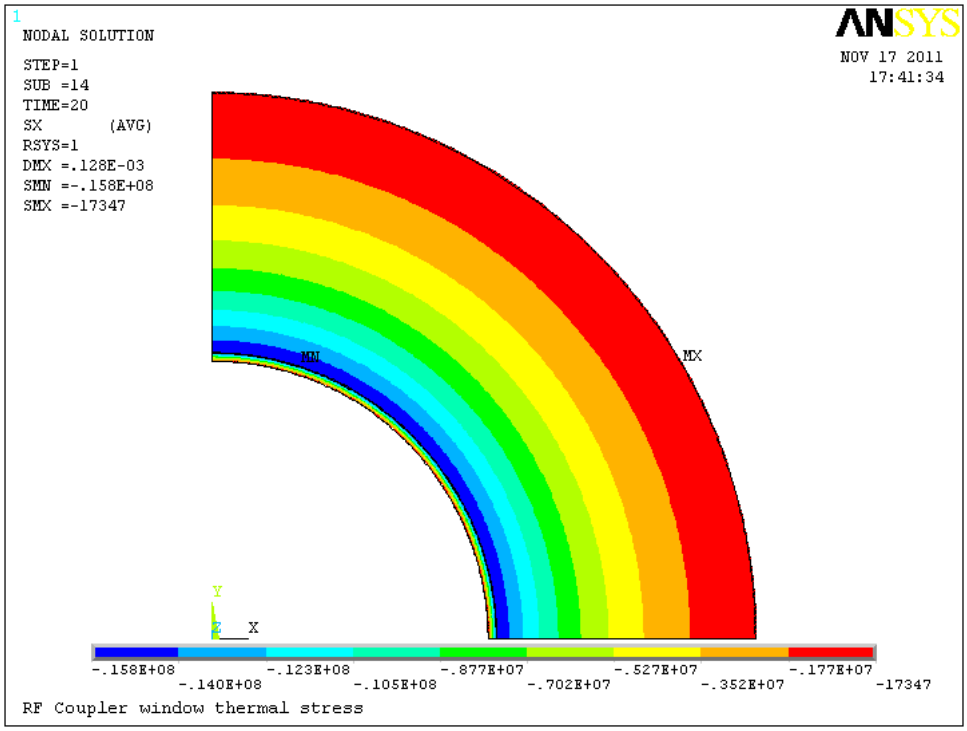

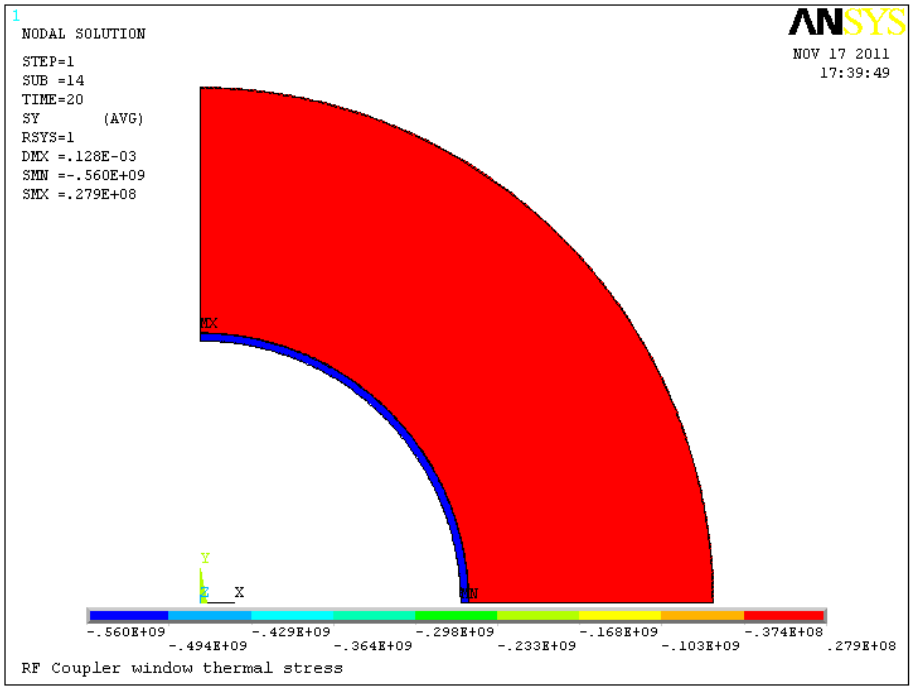

Fig.3.5a, b: Result of radial and hoop stress of plane stress model

b) Axisymmitry model with contact and target elements:

Axisymmetric solids are also called as solids of revolution. In this case, due to symmetry about circumference (θ), the displacements are confined to radial (r) and axial (z) directions only. As geometry, material properties loads and boundary conditions are axisymmetric and independent in circumferential direction, the problem is mathematically 2 D with the geometry mapped in 2D plane (r, z). In this analysis hoop normal strain ε_θ is due to radial displacement. In the present research work the ends of cylinder are free to expand. According to Hooke's law stresses σ_r (radial stress) and σ_θ (hoop stress) produces a uniform extension or contraction in z direction, and cross-sections perpendicular to the axis of cylinder remain plane. If we consider two adjacent cross-sections, the deformation undergone by the element does not interfere with the deformation of the neighboring element. Here, the elements can be considered to be in a state of plane stress.

Nonlinearity due to contact conditions are develops because the defined displacements on the boundary depend on the structure deformation. Contact between two bodies without bonding is a challenging problem. Friction between contact bodies also makes contact analysis highly nonlinear. In the present analysis node to surface contact have been generated by creating contact element 171 and target element 169.

Consider a co-axial cylinder shown in fig. 3.6 a 2D structural solid element PLANE 55 (Thermal analysis) followed by PLANE 42 (Structural analysis) is used to perform the analysis. One material model is defined. Solid modeling approach is employed. Geometric entity model is shown in fig 3.7. Maximum deflection, maximum radial and hoop stress induced in the cylinder are determined. Material properties are defined in annexure.1. Let the assumption are as followings:

- 2 D Plane stress Linear analysis
- Uniform heating
- Open end long cylinder

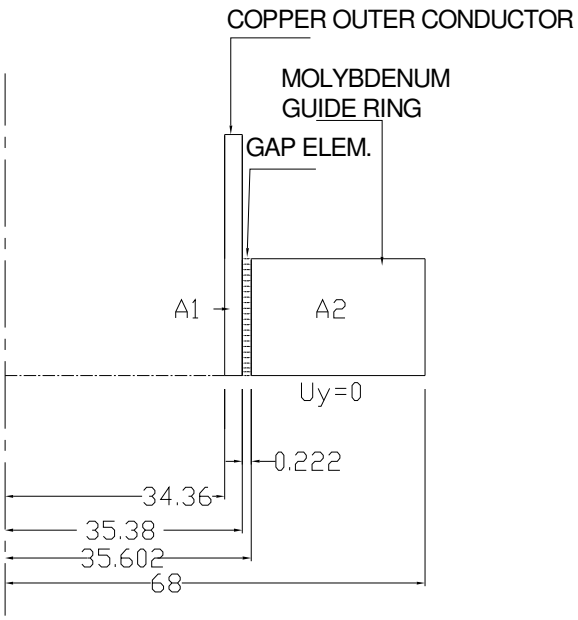

Fig.3.6: Geometric entity of axisymmetric model

- **RESULT AND DISCUSSION :**

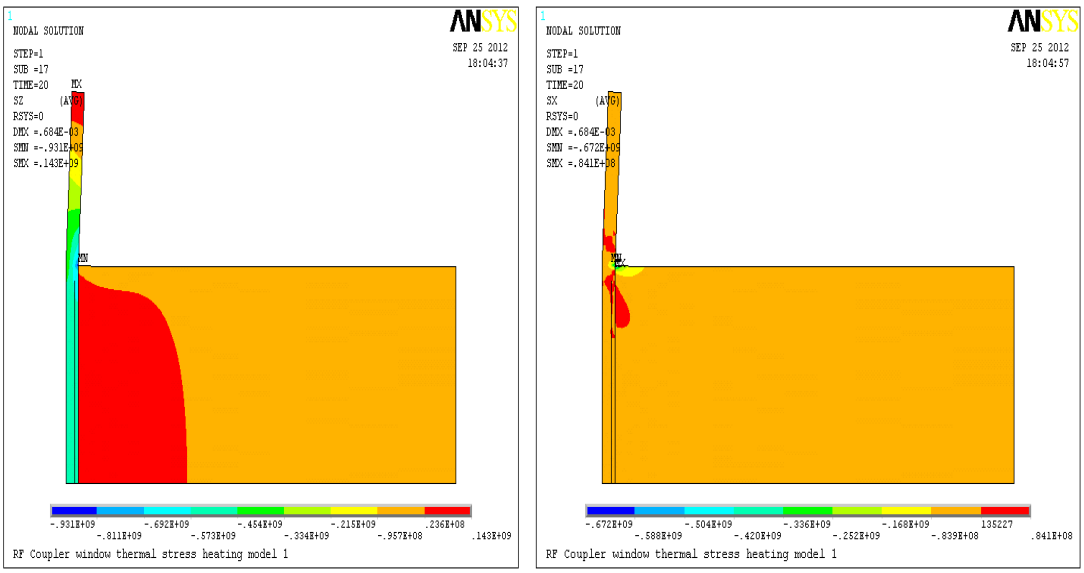

Fig.3.7 a,b,: Result of radial and hoop stress of axisymmetric model

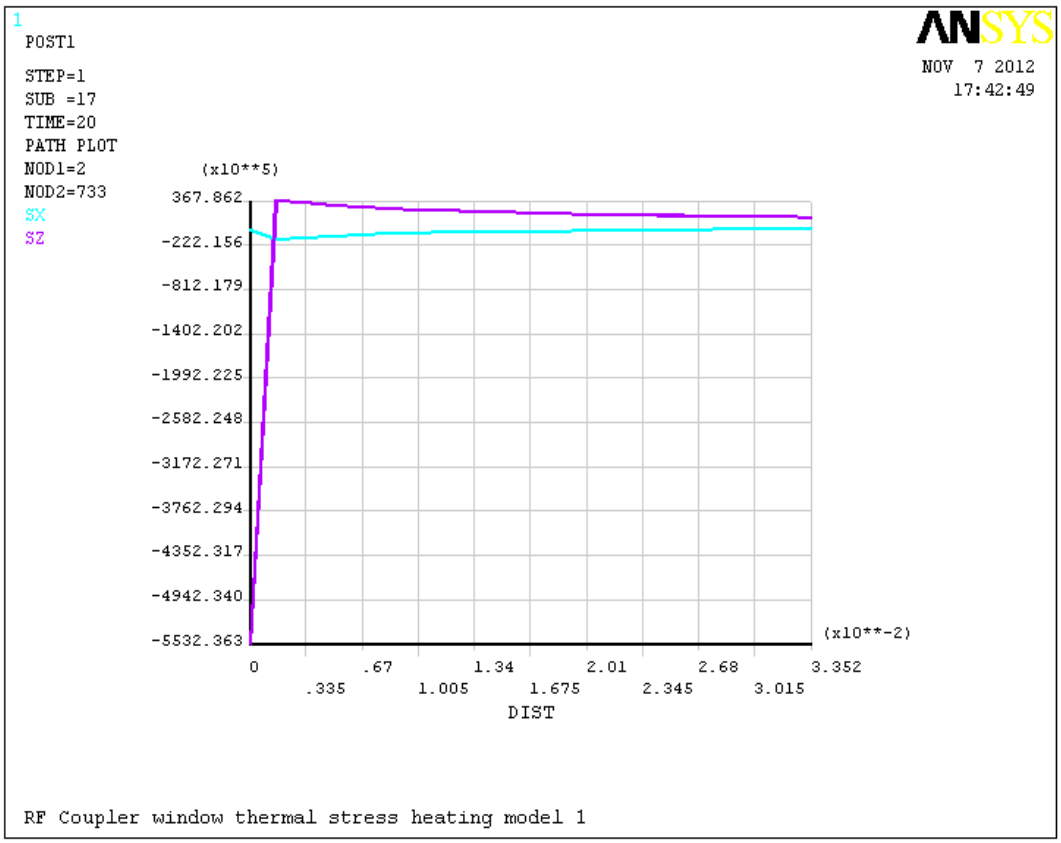

Fig.3.7,c: Result of radial and hoop stress of axisymmetric model

The results from the above plot showed that Nodal stresses of bottom nodes is matching with the result obtained from plane stress FEM code analysis results.

3.2.2.2 Thermal stress analysis results comparison obtained from analytical, plane stress and axisymmitry model of compound cylinder:

The results obtained from analytical, plane and axisymmetric Ansys simulation have been compared as followings:

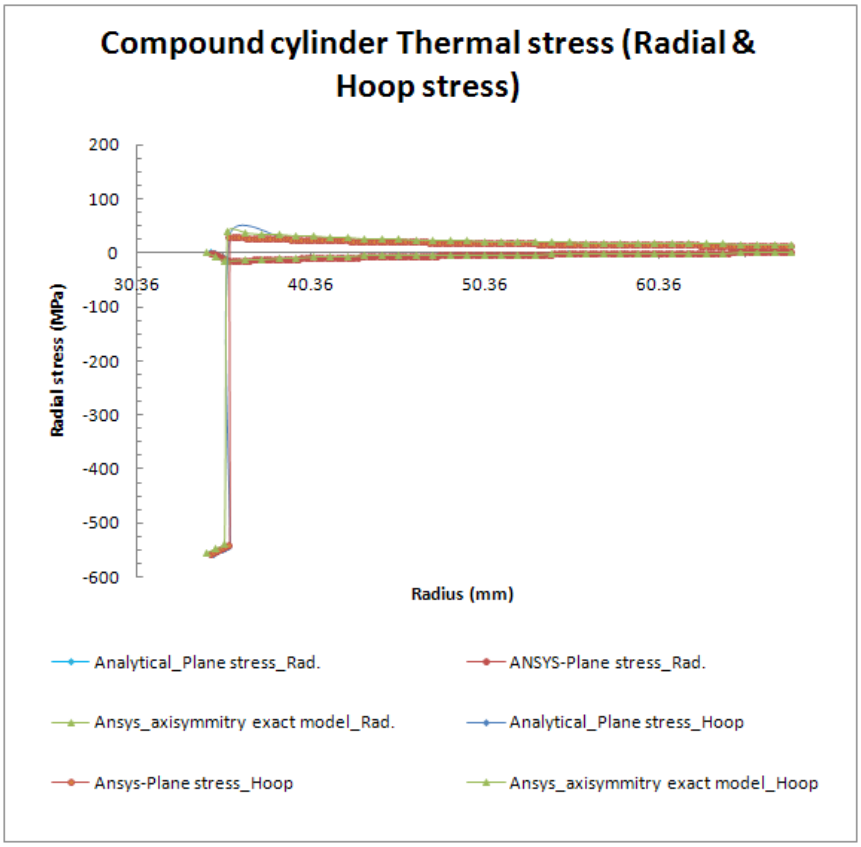

Fig.3.8: Compare plot of radial and hoop stress

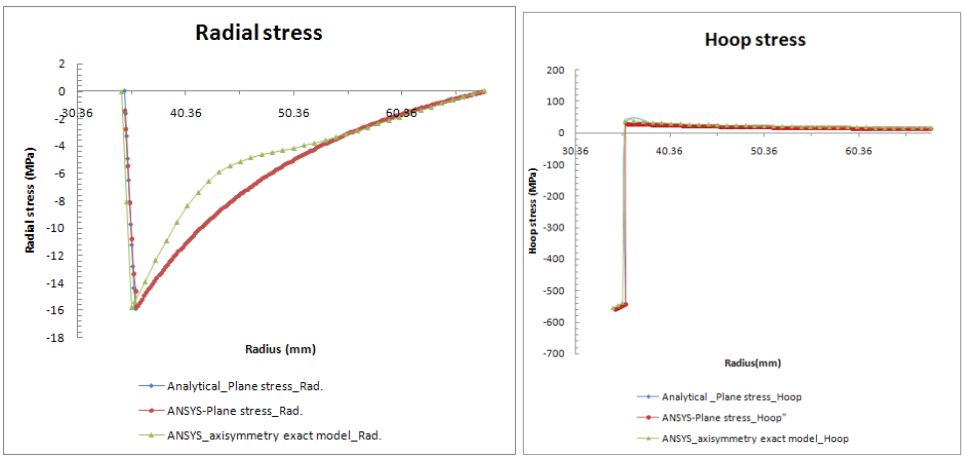

Fig.3.9 (a, b): Compare plot of radial and hoop stress (zoom view)

It revealed that results of radial and hoop stresses for all analysis are approximately same. Axisymmetric results are plotted for the bottom nodes. It is concluded here that these results shows that hoop stress value is beyond the yield limit of copper (350 Mpa).This yield will compress the inside cylinder after cooling and produces compressive stress into the alumina ceramic, which is helpful for sealing the ceramic to metal joints.

3.3 FEM - simulation for three cylinders axisymmetry model heating cycle by generating contact and target elements :

Brazing temperature filler gap has been simulated by considering another cylinder inside of model. The present model simulation needs to generate contact and target element for node to surface contact. Copper surface has been generated contact element 171 and molybdenum surface at contact point generated a target element 169. It is very complex to simulate the gap analysis. Since filler is not taking part in heating analysis so gap element generated. It activated in cooling cycle only.

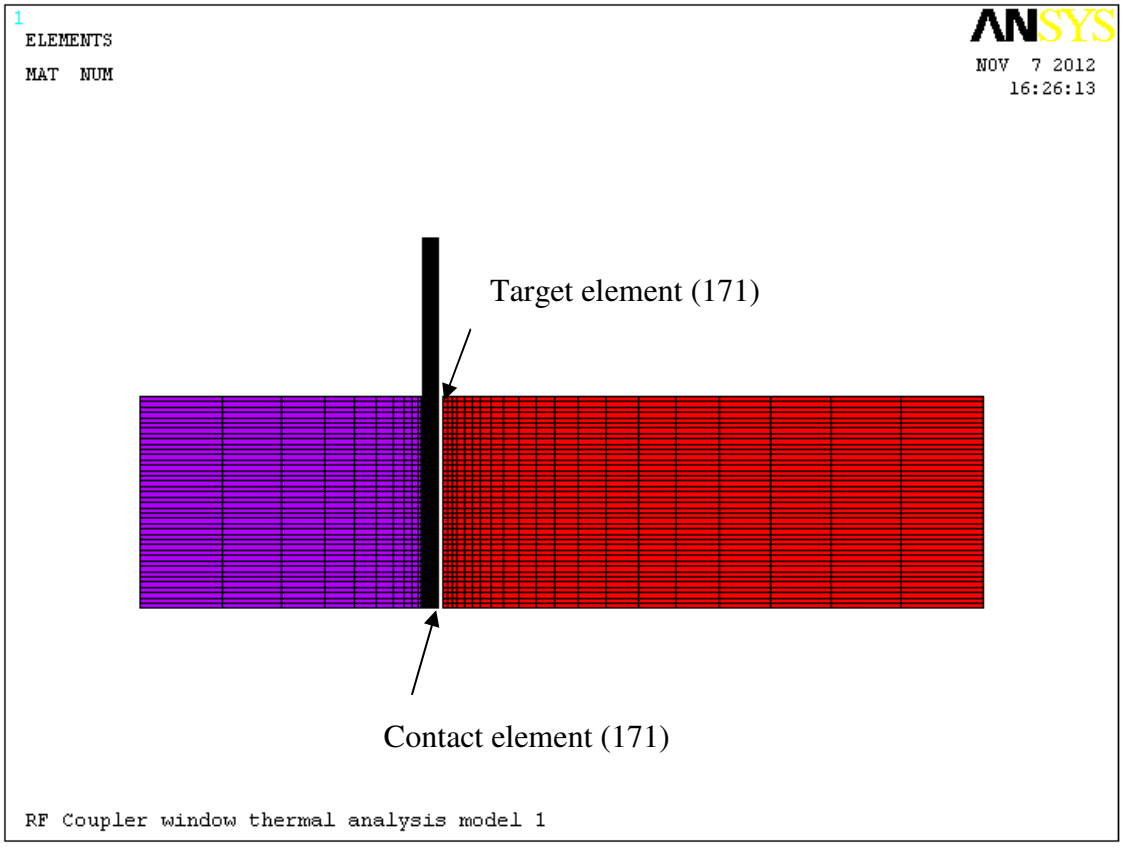

Fig.3.10: Figure of meshed element of three cylinder axisymmetry model for heating cycle

- **Result and discussion :**

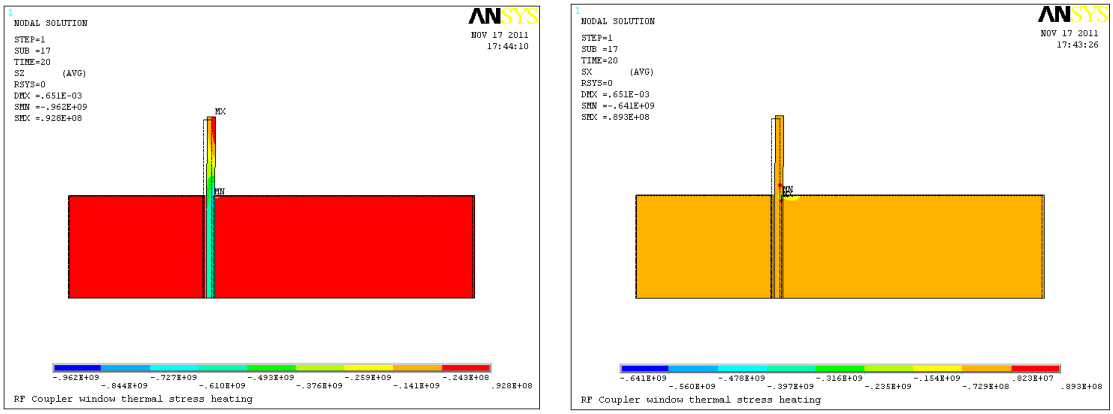

Fig.3.11 (a, b): Result of radial and hoop stress nodal solution of 2D solid model

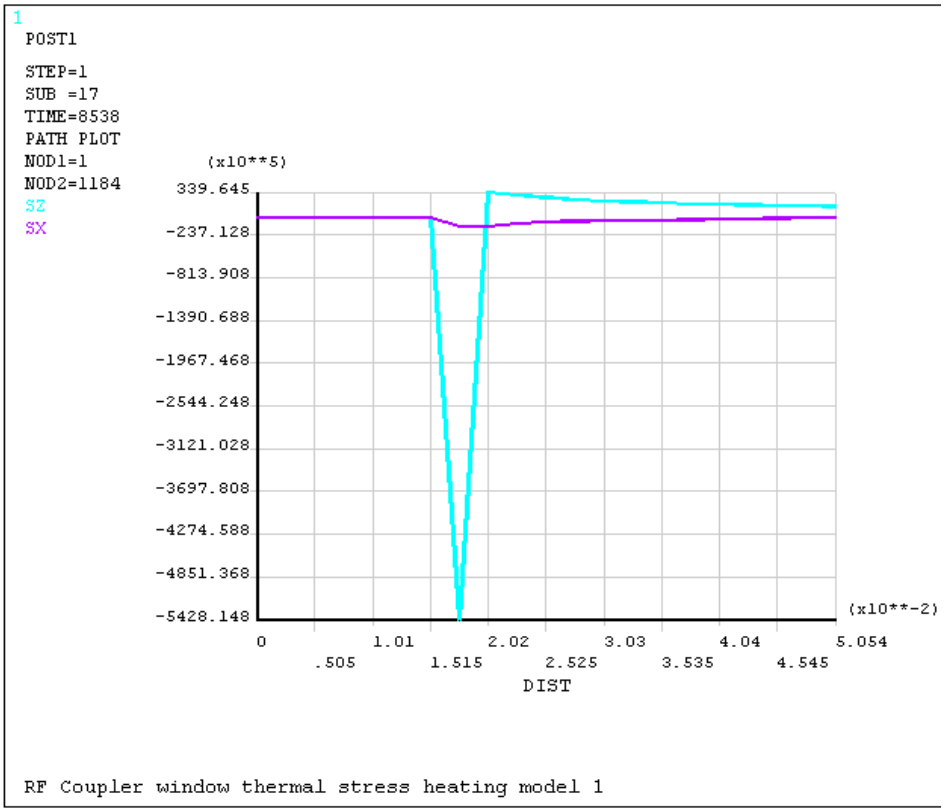

Fig.3.12: Result of radial and hoop stress by path operation

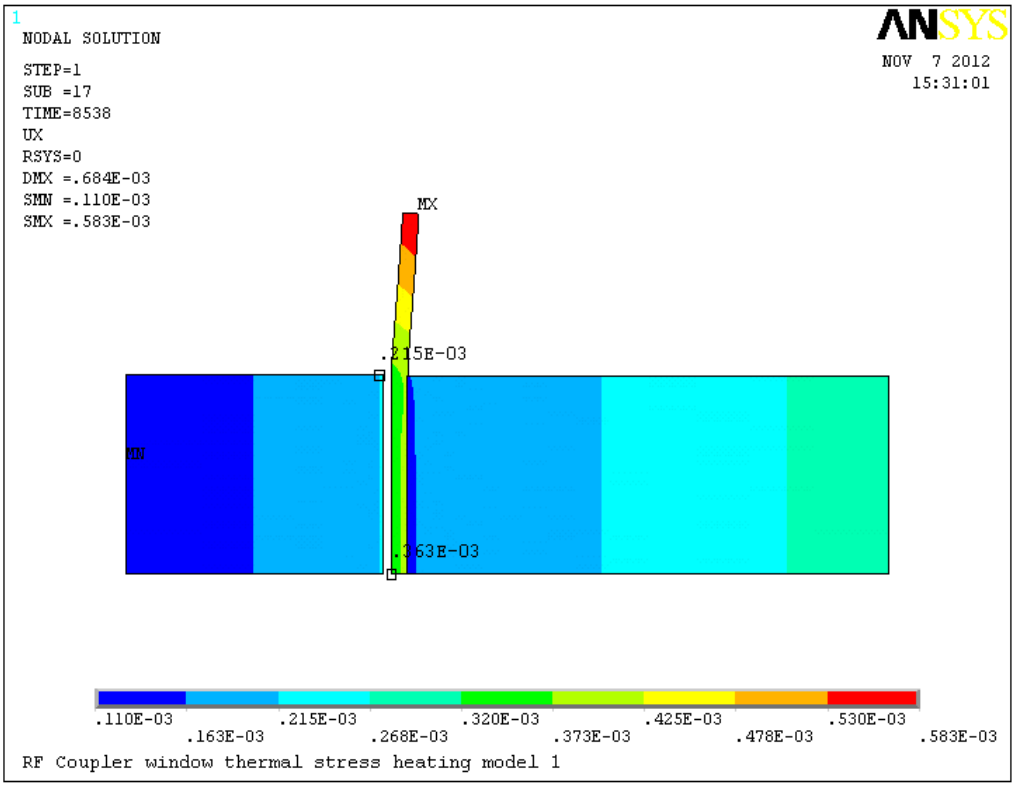

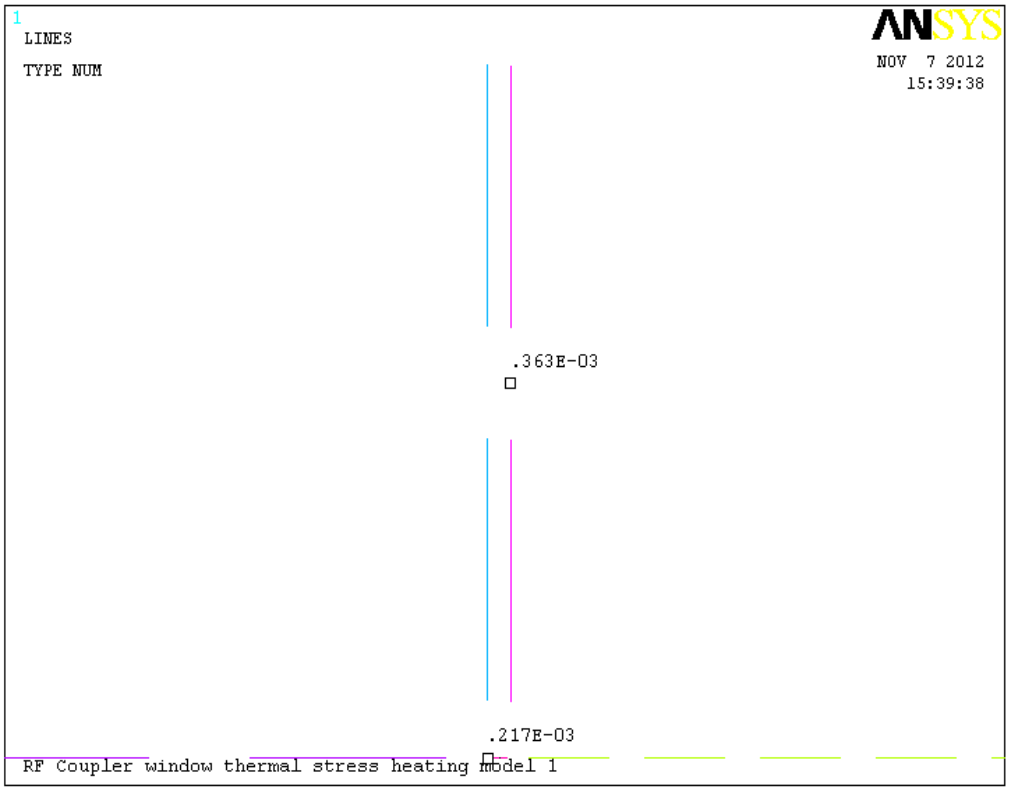

Fig.3.13 a & b: Result of deformation in radial direction of solid 2D model by path operation plot

3.4 FEM- simulation for RF window axisymmetry model using Molybdenum tooling fixture for heating and cooling cycle by generating contact and target elements (non-linear):

Ansys, a large scale general purpose finite element code, used to calculate the residual manufacturing stresses after the braze operation is completed. To solve this nonlinear problem, discrete load steps are used to account for the temperature dependent material properties and continuous plastic deformation of the braze material and copper sleeve.

3.4.1 Modeling Material Nonlinearities

A number of material-related factors can cause structure's stiffness to change during the course of an analysis. Nonlinear stress-strain relationships of plastic, multilinear *elastic,* and *hyper elastic* materials will cause a structure's stiffness to change at different load levels (and, typically, at different temperatures). Creep, viscoplasticity, and viscoelasticity will give rise to nonlinearities that can be time-, rate-, temperature-, and stress-related. *Swelling* will induce strains that can be a function of temperature, time, neutron flux level (or some analogous quantity), and stress. Any of these kinds of material properties can be incorporated into an ANSYS analysis if use appropriate element types. Nonlinear constitutive models (TB command, except for TB, FAIL) are not applicable for the ANSYS Professional program.

3.4.1.1 Nonlinear Materials

If a material displays nonlinear or rate-dependent stress-strain behavior, then it must use the TB family of commands to define the nonlinear material property relationships in terms of a data table. The exact form of these commands varies depending on the type of nonlinear material behavior being defined.

3.4.1.2 Plasticity

Most common engineering materials exhibit a linear stress-strain relationship up to a stress level known as the proportional limit. Beyond this limit, the stress-strain relationship will become nonlinear, but will not necessarily become inelastic. Plastic behavior, characterized by nonrecoverable strain, begins when stresses exceed the material's *yield point*. Because there is usually little difference between the yield point and the proportional limit, the ANSYS program assumes that these two points are coincident in plasticity analyses.

Plasticity is a nonconservative, path-dependent phenomenon. In other words, the sequence in which loads are applied and in which plastic responses occur affects the final solution results. If you anticipate plastic response in your analysis, you should apply loads as a series of small incremental load steps or time steps, so that your model will follow the load-response path as closely as possible. [34]

3.4.1.3 Bilinear Kinematic Hardening

The **Bilinear Kinematic Hardening** (BKIN) option assumes the total stress range is equal to twice the yield stress, so that the Bauschinger effect. This option is recommended for general small-strain use for materials that obey von Misses yield criteria (which includes most metals). It is not recommended for large-strain applications.

Von Mises material models are available for 2-D, beam, shell, brick and tetrahedral elements. These material models are used when an elastic material is loaded beyond the yield strength of the material. When this occurs, plastic deformation takes place. The von Mises with hardening material model will use a bilinear curve to calculate the stress value. In the elastic region stress and strain curve has a slope equal to modulas of elasticity, and in plastic region stress and strain curve has a slope equal to strain hardening modulas (Tangent modulas).

There are two types of hardening material models available. The isotropic hardening model involves yielding the entire yield surface uniformly. The kinematic hardening involves shifting of the yield surface due to reversal of load. The kinematic hardening model preferred for analysis involve cyclic loading (Bauschinger effect). In this research work BKIN command used for nonlinear analysis of FEM model.[34]

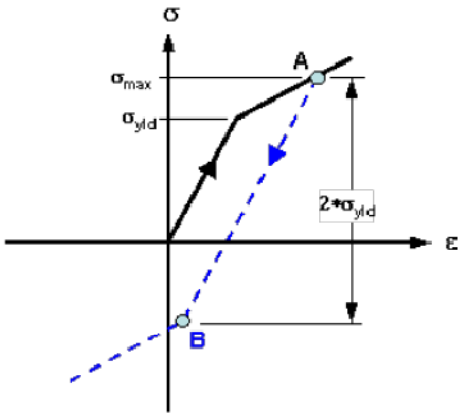

Fig.3.14: Figure of Bauschinger effect

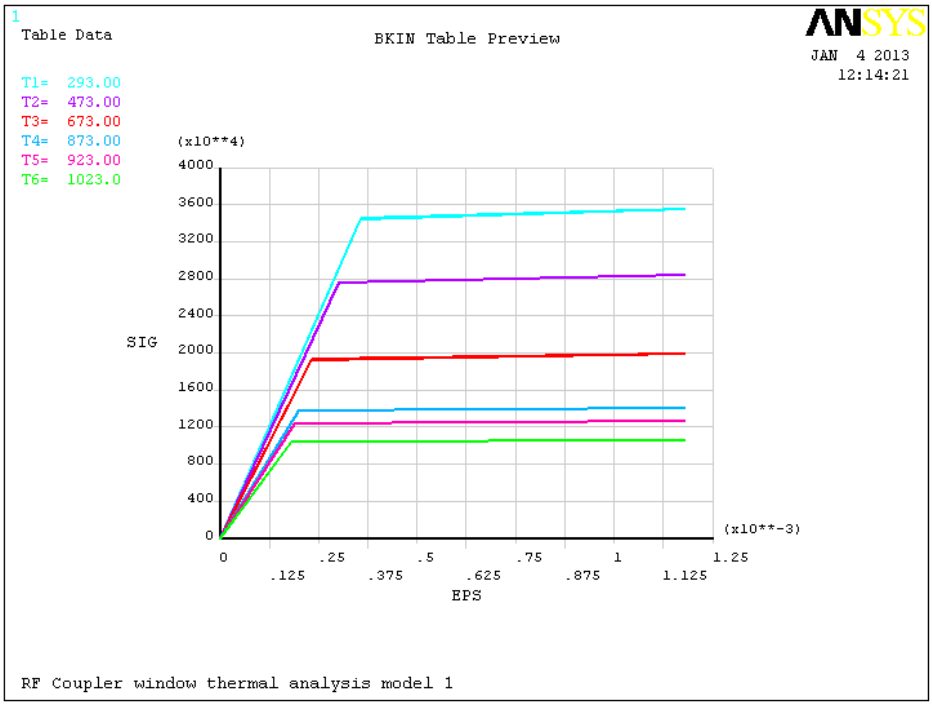

Fig.3.15: Plot of stress strain curve of elasto-plastic with strain hardening of Cu., obtain from ansys material model by BKIN properties

3.4.1.4 Temperature - Dependent Coefficient of thermal expansion of copper & Molybdenum

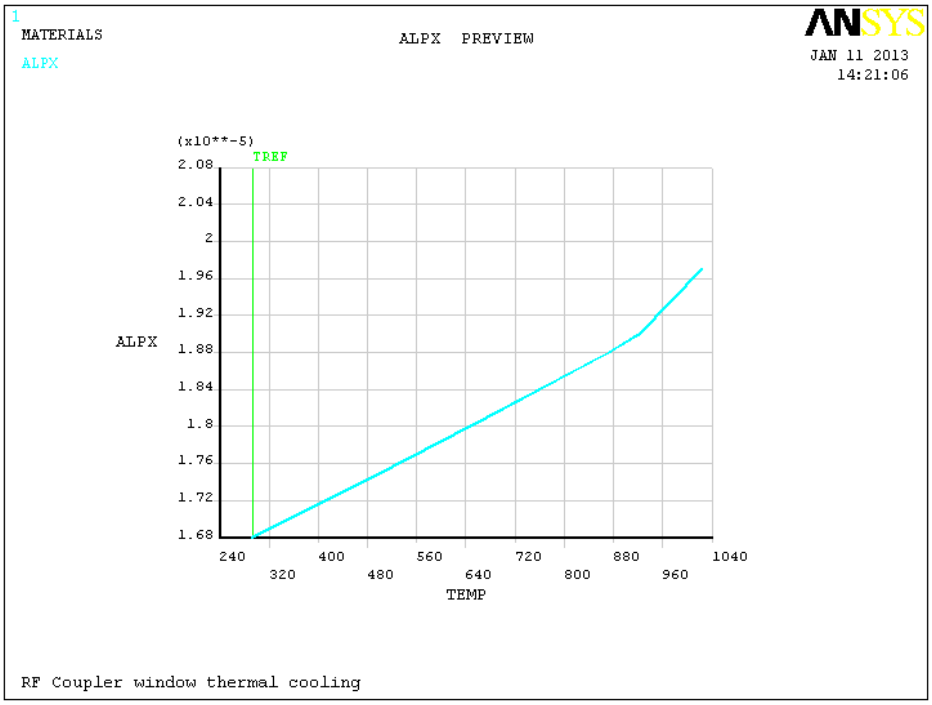

Fig.3.16 :Temperature dependent $\alpha^{cu}$of copper from ansys material model

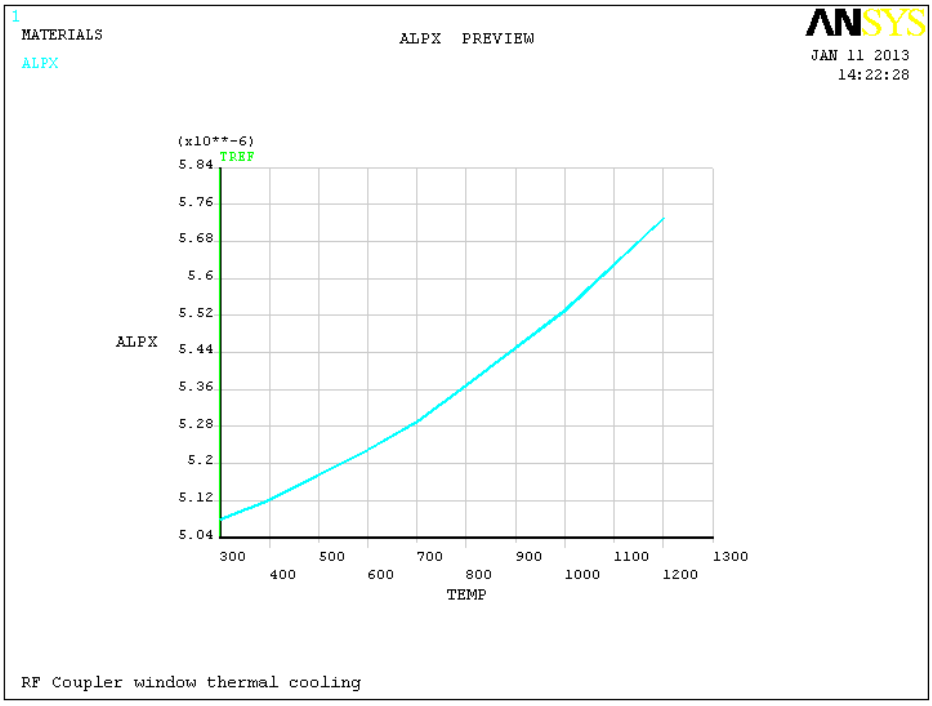

Fig.3.17: Temperature dependent $\alpha^{Mo.}$ of Molybdenum from ansys material model

3.4.1.5 Braze material Non-linear properties

In the R.F window, ceramic to metal furnace brazing process tooling fixture is required to restrained the thermal growth of the copper sleeve to control the braze gap. This causes the initial compression of copper sleeve in the radial and hoop direction during heating cycle, which is not relieved when the braze flows. To account for this, a simulation of both the heating and cooling phases has to be performed. TREF for ceramic, copper and tooling fixture in heating cycle is room temperature. The braze material is not acted any part during heating cycle but it is needed in the cooling cycle of the analysis, so elements cannot be added in the restart. When the braze flows and solidifies, the braze solidus temperature becomes it zero-strain reference temperature.[2]

3.4.1.5.1 Estimstion of Temperature - Dependent Coefficient of thermal expansion for different zero strain points :

If the part initial temperature state (P1), is different from the material referance temperature state (Po), then the $\propto$s values must be modified. The subscript RM means ‘ reference material’ , and subscript RP means ‘ reference part,. Fig. 2 graphically depicts the computational method.

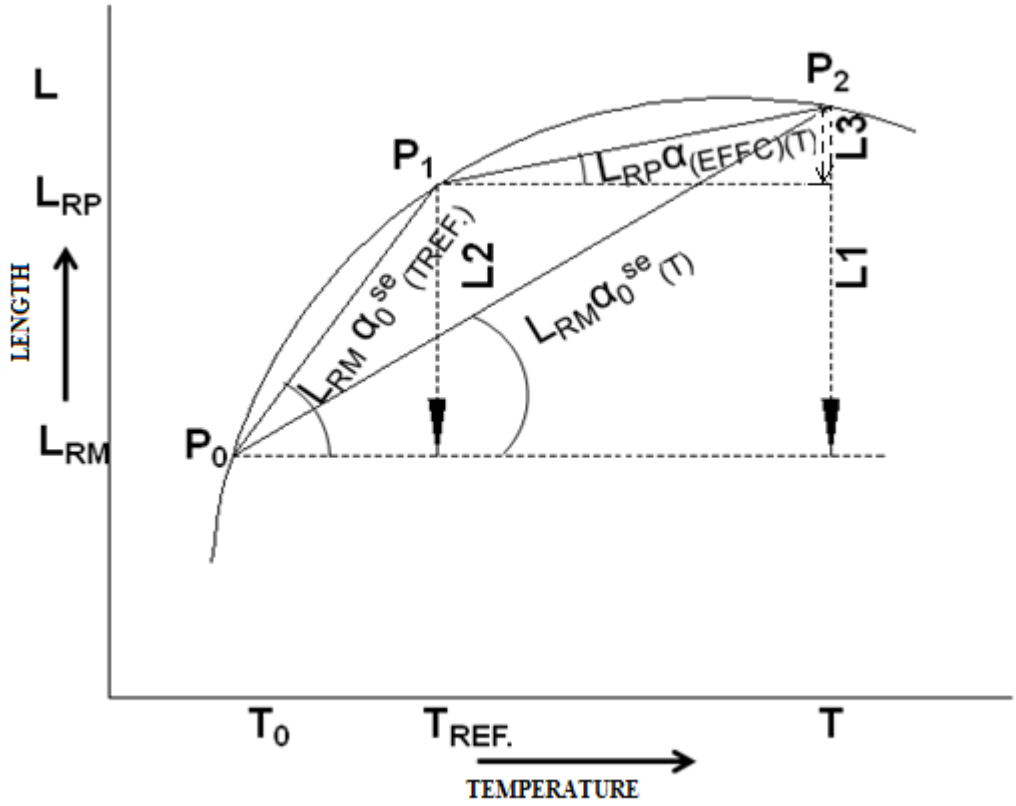

Fig.3.18 : Interpolation of temperature dependent modified $\alpha^{Cusil}$of braze filler

(T_0, L_{RM}) is the reference state at point P_0. This is material reference state data. $\propto_O^{se}{}_{(TREF)}$ is the secant coefficient of expansion at temperature, $T_{REF.}$ $\propto_O^{se}{}_{(T)}$ is the secant coefficient of expansion at temperature, T. $\propto_O^{se}{}_{(TREF.)}$ and $\propto_O^{se}{}_{(T)}$ are obtained from material properties data book.

($T_{REF.}$, L_{RP}) is the part reference state point P_1 . This is the zero thermal strain point at initial temperature need to find $\propto_{EFFC.}$ For other temperatures $\propto_{se}$.

$L_{RM}\propto_O^{se}{}_{(To)}$ is the slope of the line from point P_0 to P_1

$L_{RM}\propto_O^{se}{}_{(T).}$ is the slope of the line from point P_0 to P_2

$L_{RP.}\propto_{EFFC(T).}$ is the slope of the line from point P_1 to P_2

$L1 = L - L_{RM} = L_{RM} . \propto_O^{se}{}_{(T)..} . (T - T_O)$ -------- (1)

$\varepsilon_1 = L1 / L_{RM} = \propto_O^{se}{}_{(T)..} . (T_. - T_O)$ -------- (2)

$L2 = L_{RP} - L_{RM} = L_{RM} . \propto_O^{se}{}_{(TREF.)} . (T_{REF.} - T_O)$ -------- (3)

$\varepsilon_2 = L2/ L_{RM} = \propto_O^{se}{}_{(TREF.)} . (T_{REF.} - T_O)$ --------(4)

$L3 = L - L_{RP} = L_{RP} . \propto_{EFFC(T).} . (T - _{TREF.})$ --------(5)

$\varepsilon_3 = L3/ L_{RP} = \propto_{EFFC(T)} . (T - _{TREF.})$ --------(6)

since, L3 = L1 – L2 from Fig.1

$\therefore\ L_{RP} . \propto_{EFFC(T)} . (T - _{TREF.}) = L_{RM} . \propto_O^{se}{}_{(T)..} . (T - T_O) - L_{RM} . \propto_O^{se}{}_{(TREF.)} . (T_{REF.} - T_O)$

or $$\alpha_{EFFC.(T)} = \frac{L_{RM}}{L_{RP}} . \frac{\left(\alpha^{se}_{0(T)} . (T - T_o) - \alpha^{se}_{0(TREF)} . (T_{(REF.)} - T_o)\right)}{(T - T_{REF.})}$$

or $$\alpha_{EFFC.(T)} = \frac{L_{RM}}{L_{RP}} . \frac{\left(\alpha^{se}_{0(T)} . (T - T_{REF.} + T_{REF.} - T_o) - \alpha^{se}_{0(TREF)} . (T_{(REF.)} - T_o)\right)}{(T - T_{REF.})}$$

or $$\alpha_{EFFC(T)} = \frac{L_{RM}}{L_{RP}} . (\alpha^{se}_{0(T)} + \frac{(T_{(REF.)} - T_o)}{(T - T_{REF.})} . (\alpha^{se}_{0(T)} - \alpha^{se}_{0(TREF)}))$$

when, $L_{RP} \cong L_{RM}$, $\alpha_{EFFC(T)} = \alpha^{se}_{0(T)} + \frac{(T_{(REF.)} - T_o)}{(T - T_{REF.})} . (\alpha^{se}_{0(T)} - \alpha^{se}_{0(TREF)})$ ------ (7)

The approach in ANSYS to it is required to link heating and cooling brazing phase. The piece parts in the braze furnace have a TREF at room temperature whole the braze material's TREF is at the braze solidus temperature. This problem may be resolved by leaving the TREF parameter set at room temperature (set during heating phase) and only modifying the $\propto_{EFFC.(T)}$ table for the braze material by following equation.

Braze material during cool down :

$$\in_{THERMAL(COMPUTER)} = \in_{THERMAL(ACTUAL)}$$

$$\alpha_{EFFC.(T)TREF=T_{ROOM}} X (T - T_{ROOM}) = \alpha_{EFFC.(T)TREF=T_{BRAZE}} X (T - T_{BRAZE}) \quad \text{-- (8), (9), (10)}$$

$$\alpha_{EFFC.(T)TREF=T_{ROOM}} = \alpha_{EFFC.(T)TREF=T_{BRAZE}} X \frac{(T - T_{BRAZE})}{(T - T_{ROOM})}$$

After calculating $\propto_{EFFC.(T)}$ for the braze material using eq. (7) based on a TREF equal to the braze solidus temperature. Using eq. (10) generate a modified $\propto_{EFFC.\ (T)TREF=Troom}$ for braze material, which can be used with the current TREF, but reflect the braze material's actual TREF at the braze solidus temperature. In calculating an $\propto_{EFFC.(T)}$ table T equal to TREF has not been used. A discontinuity exists in eq. (10) as T approaches TREF. Instead, it is used T equal to TREF $\pm$ 1. [2]

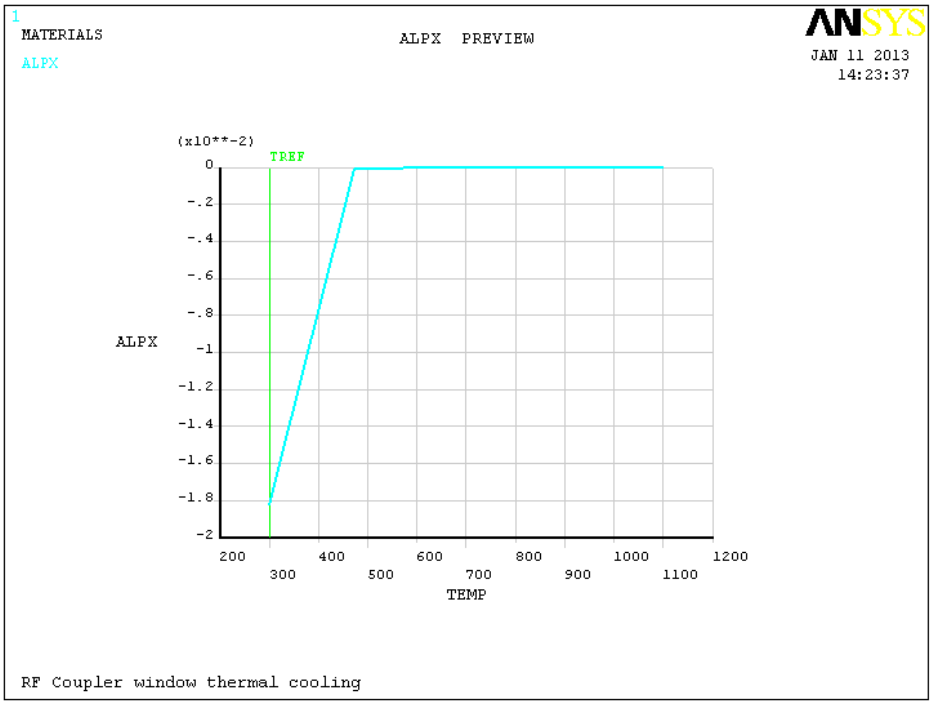

Fig.3.19: Plot of Temperature dependent modified α^{Cusil} of braze filler from ansys material model

3.4.1.6 Result and discussion :

The coefficient of linear thermal expansion of cusil of $T_{ref.}$ at room temperature from fig. 3.19 shows that negative value from room to brazing temperature. During cooling this value will automatic modified all value during simulation of cooling cycle.

Fig.3.20 :Picture of axisymmetry FEM model elements view from Ansys.

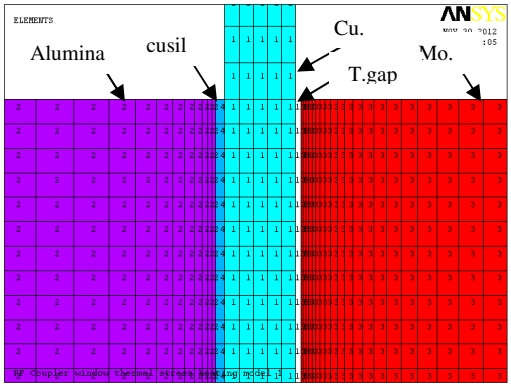

Fig.3.21a

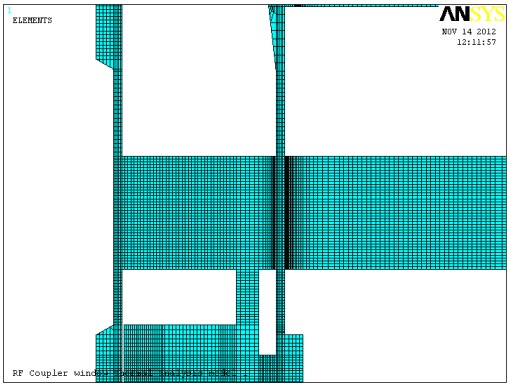

Fig.3.21b

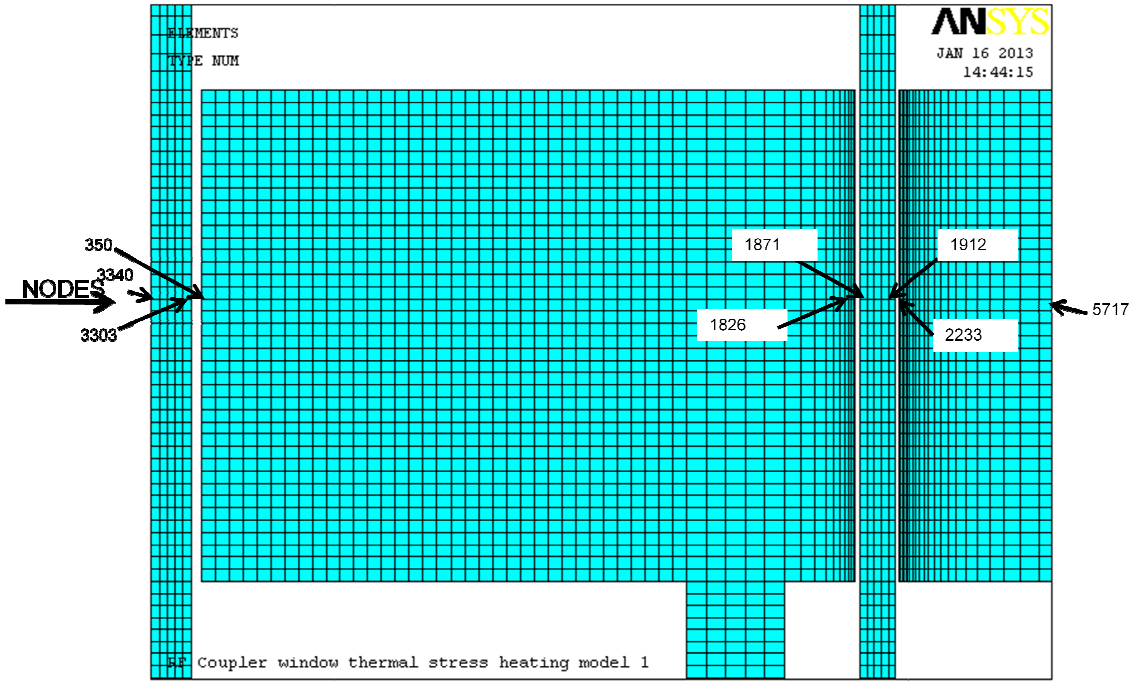

Fig.3.21c : Picture of axisymmetric FEM model element & material model zoom view from ansys

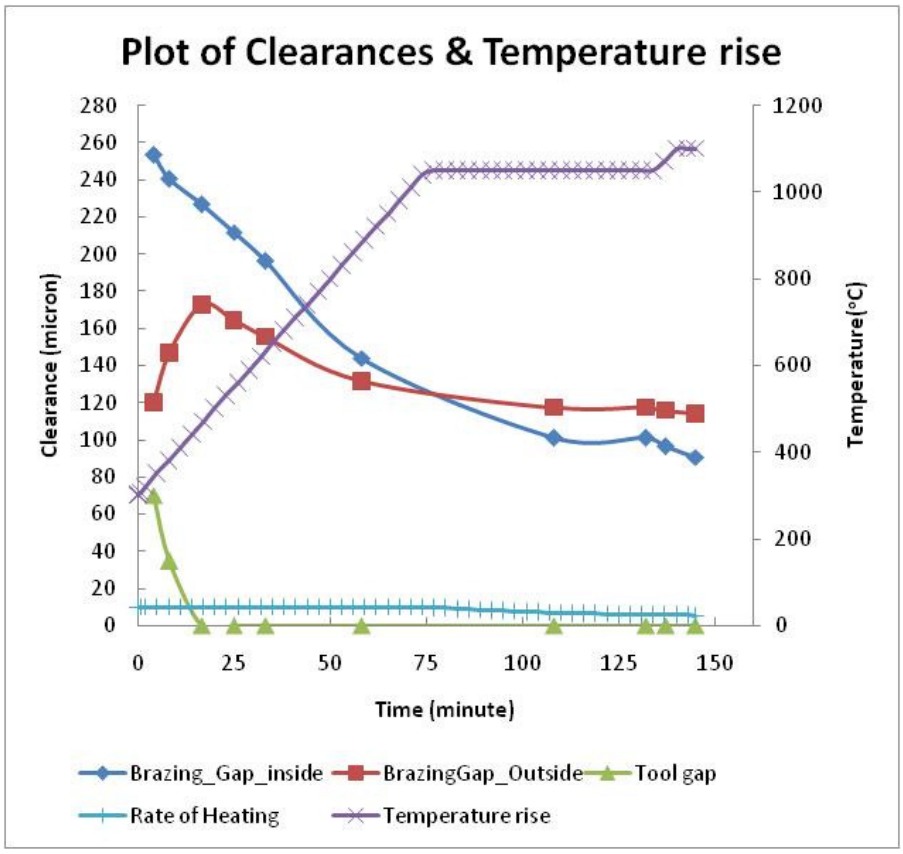

Fig.3.22: Plot of Heating cycle, trend of clearance and temperature

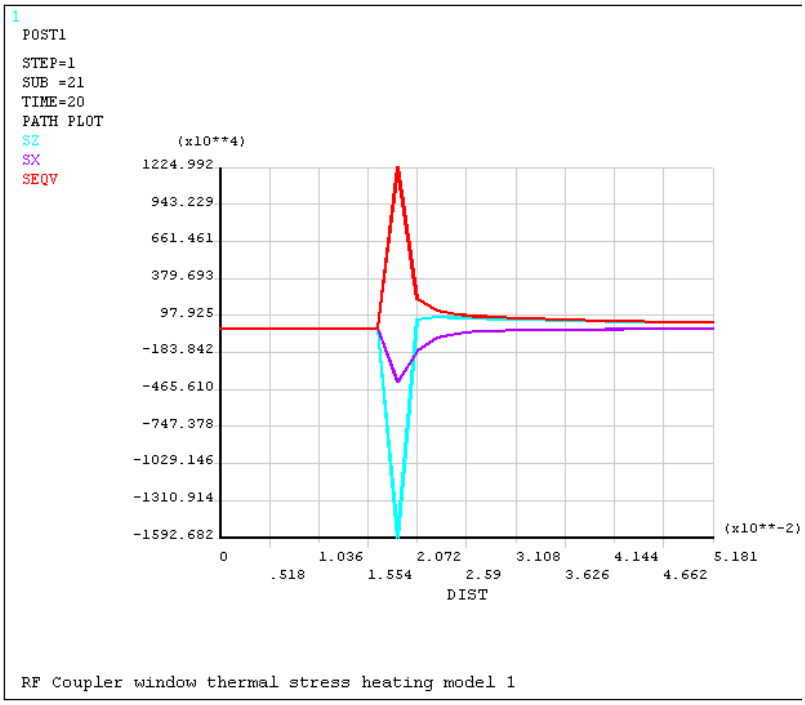

Fig.3.23: Plot of result for radial, hoop and von mises stress by path operation of heating cycle

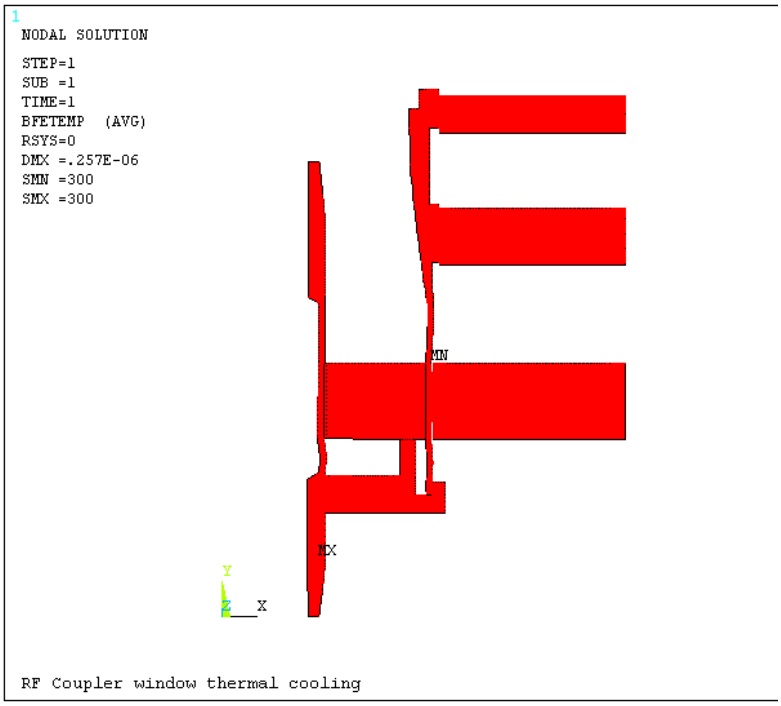

Fig.3.24a: Plot of nodal temperature of cooling cycle

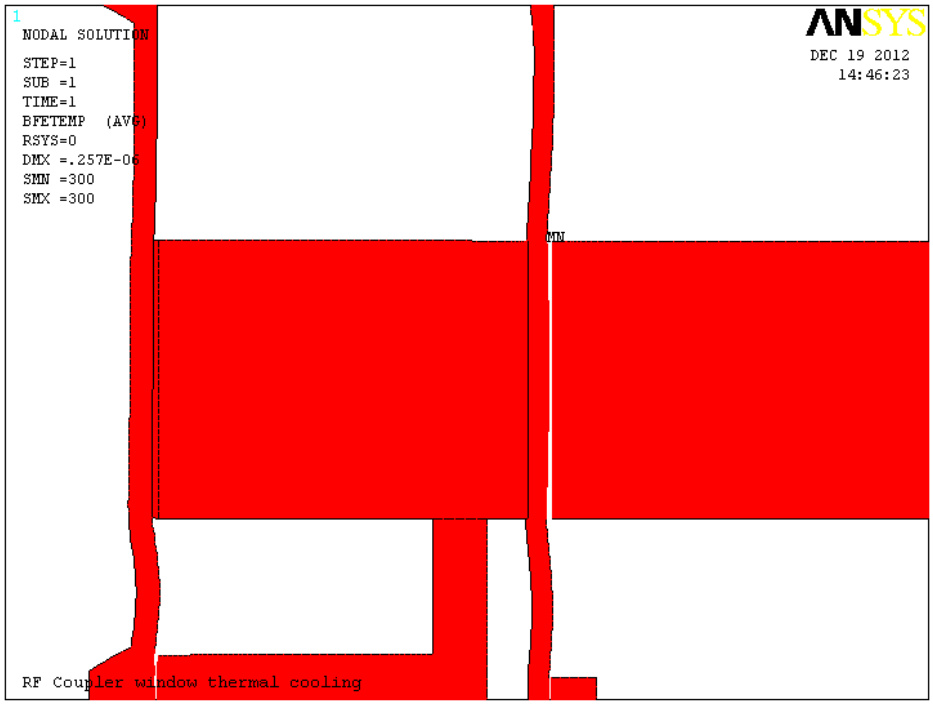

Fig.3.24b: Plot of nodal temperature of cooling cycle zoom view

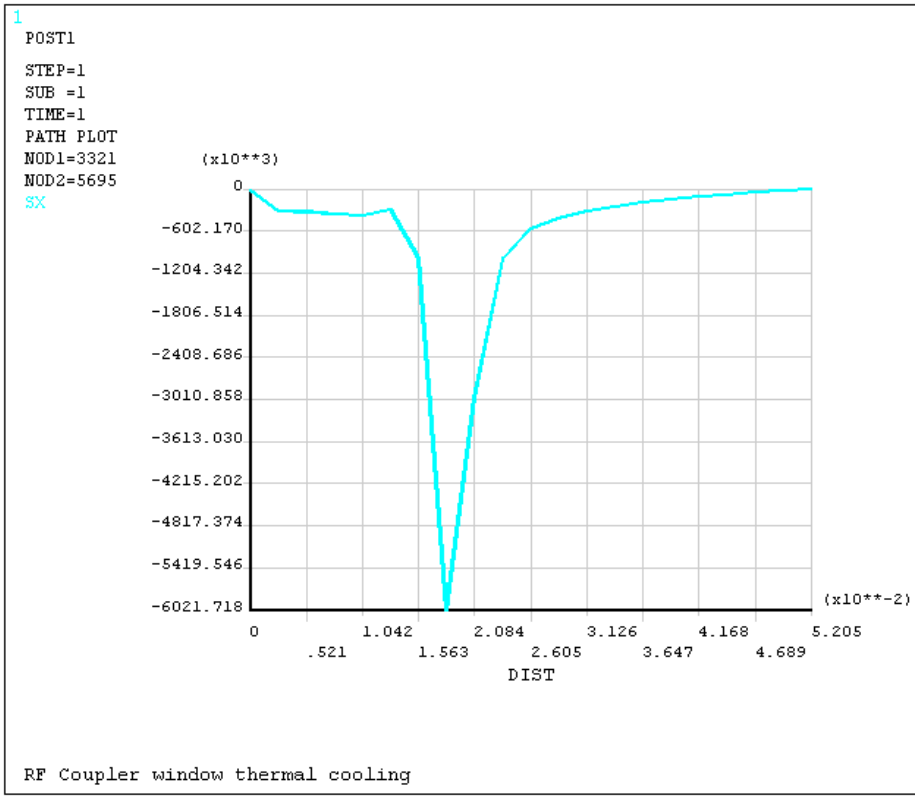

Fig.3.25: Plot of radial stress of cooling cycle

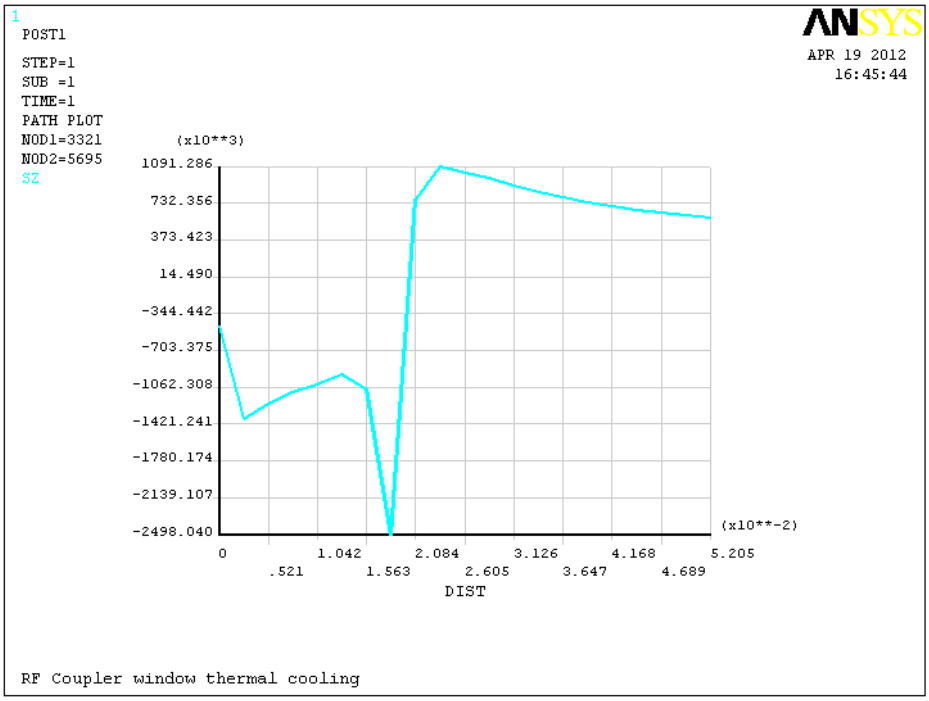

Fig.3.26 Plot of hoop stress of cooling cycle

3.5 FEM - simulation for fabrication trial of outer brazing joint model using graphite tooling fixture:

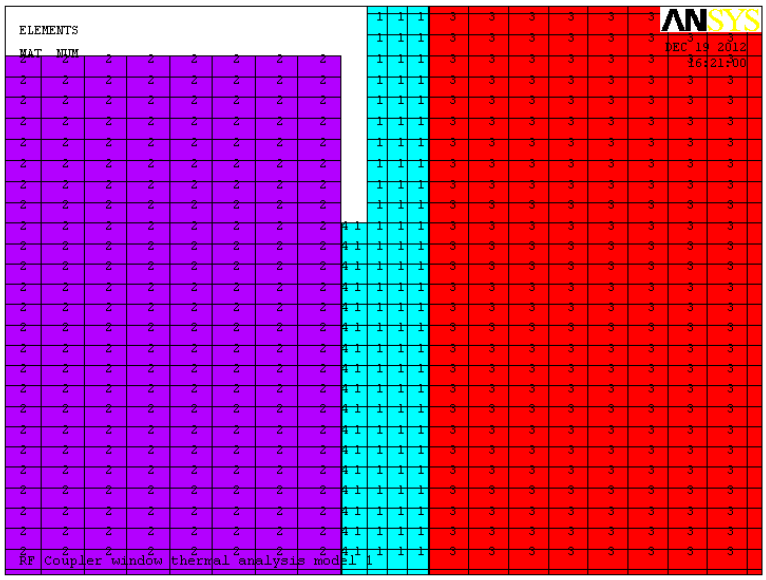

Fig.3.27 Plot of Graphite tooling fixture with test model element view from material model

ELEMENT No.	MATERIAL DESCRIPTION		NODES NO.		
			Bottom	Middle	Top
1	OFHC COPPER	I.D	3158	5327	5302
		O.D	3186	5371	5346
2	ALUMINA 300	I.D	-	3764	-
		O.D	3998	4051	4026
3	PYROLYTIC GRAPHITE	I.D	5478	5578	5538
		O.D	3270	6268	6242
4	CUSIL FILLER	I.D	3998	4051	4026
		O.D	3158	5327	5302

Table 3.2 : Test model element materials description

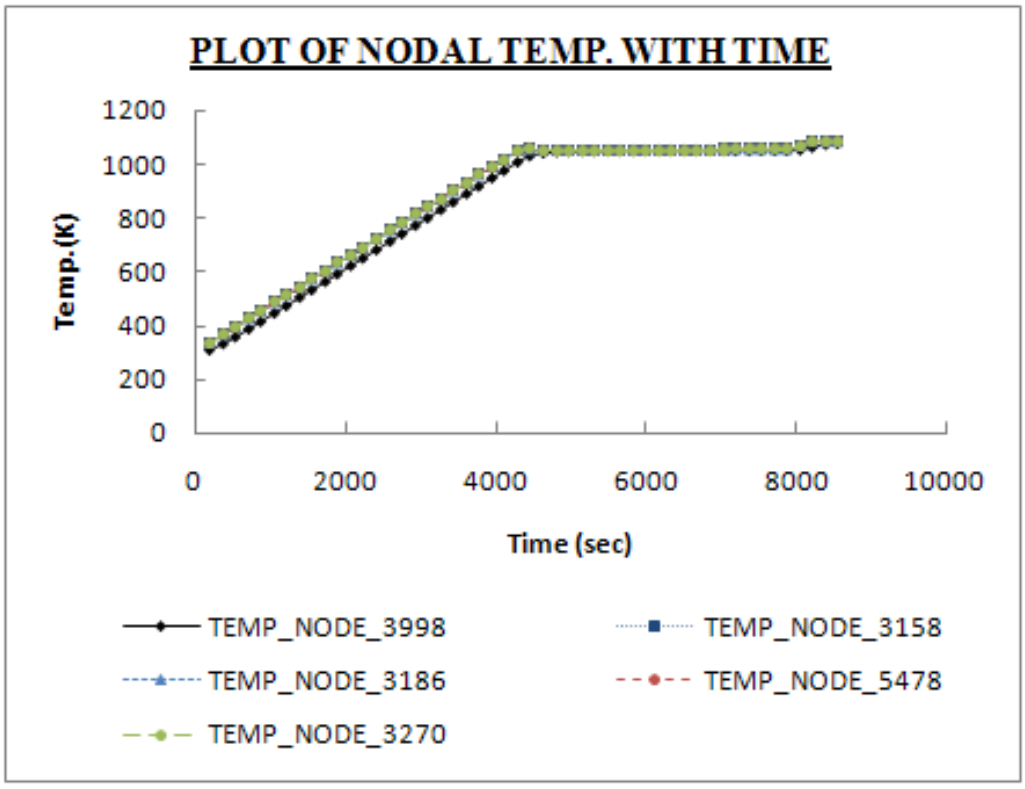

Fig.3.28 : Plot of nodal temperature of graphite tooling fixture with test model

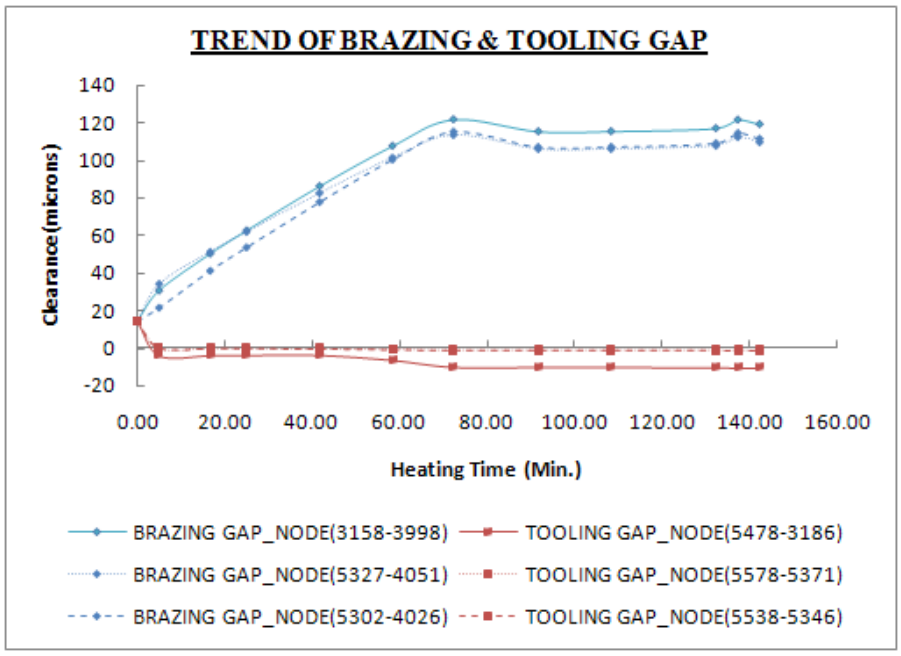

Fig.3.29:Plot of Heating cycle , trend of clearance of graphite tooling fixture with test model

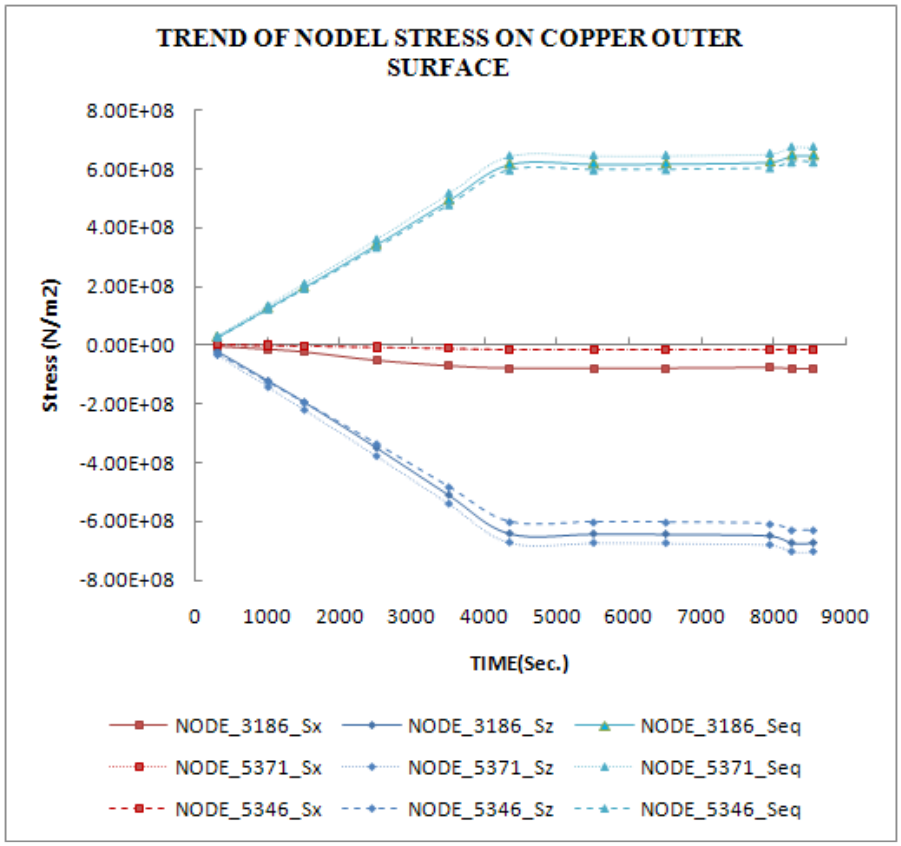

Fig.3.30: Plot of nodal solution result of radial, hoop and von mises stress for Copper of heating cycle (Graphite tooling fixture with test model)

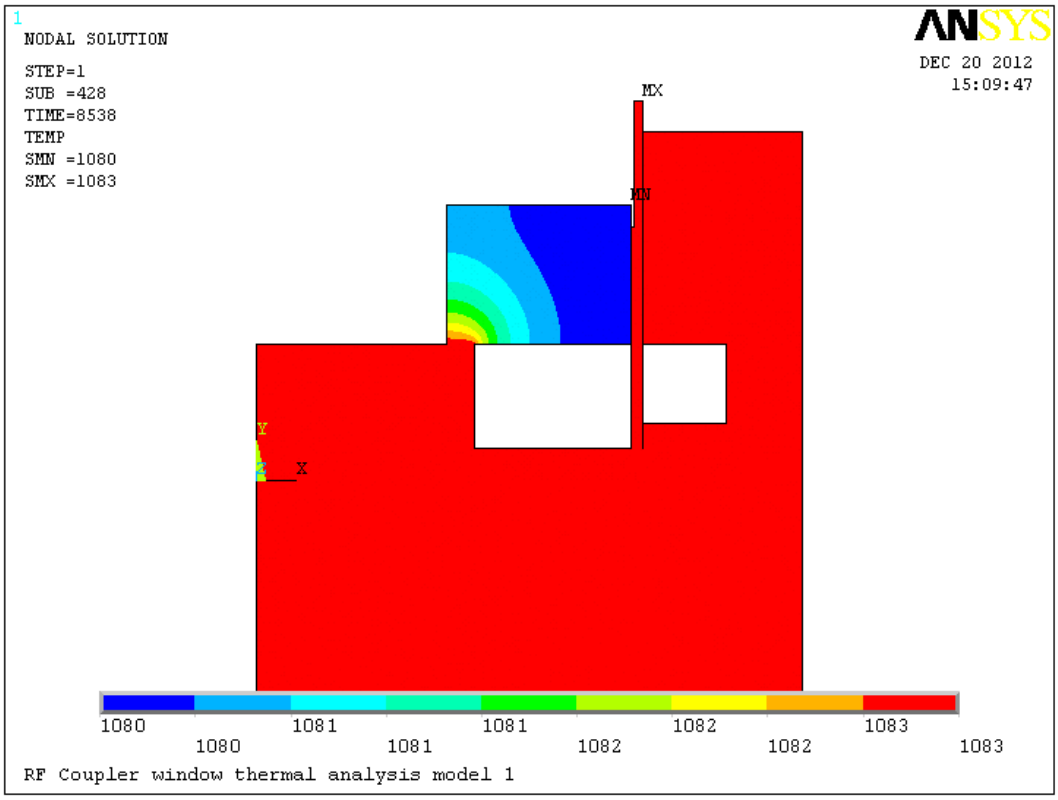

Fig.3.31: Plot of nodal temperature by flux heating (Graphite tooling fixture with test model)

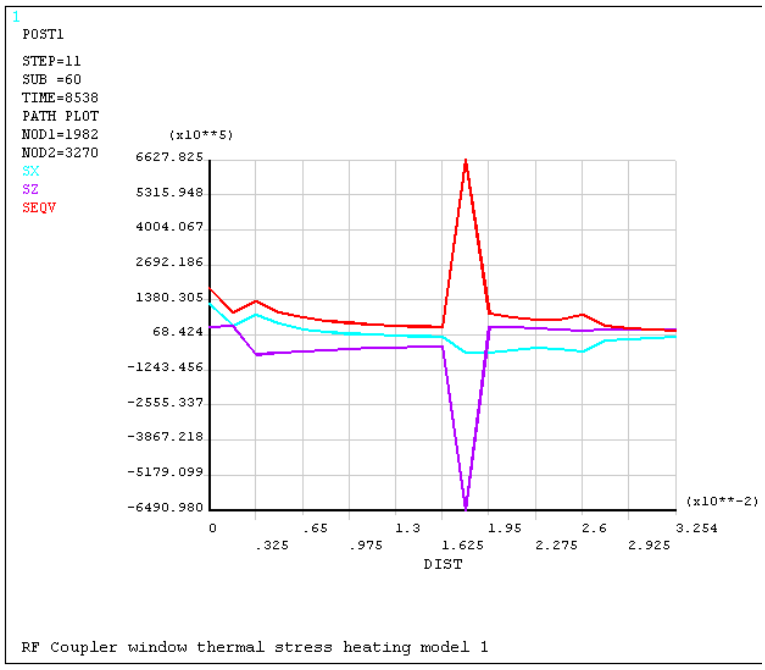

Fig.3.32: Plot of stresses of heating cycle by path operation (Graphite tooling fixture with test model)

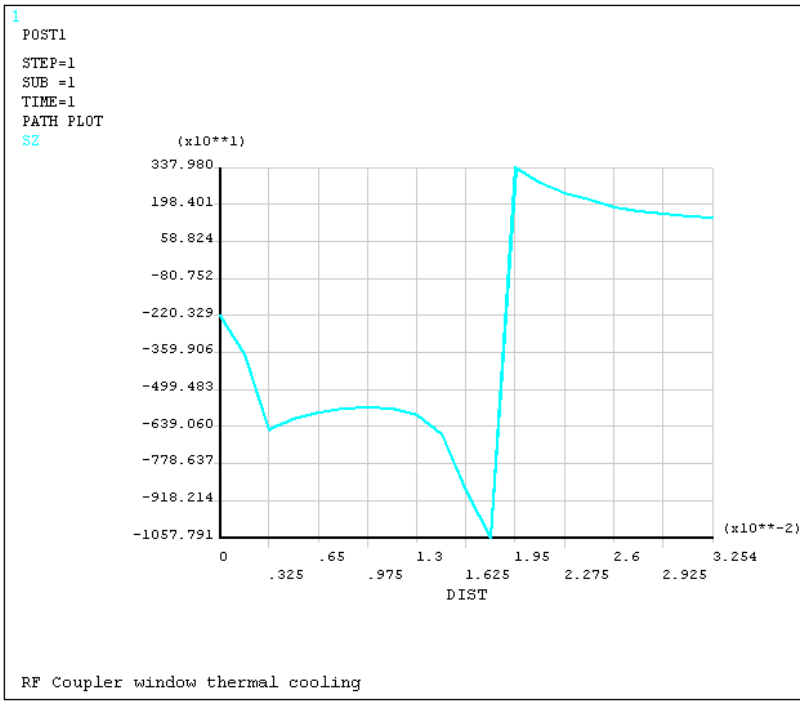

Fig.3.33: Plot of nodal solution for hoop stress of cooling cycle by path operation (Graphite tooling fixture with test model)

From fig. 3.33 we can see that hoop stress after cooling is less than the allowable stress. Based on the dimensions of design value drawing of fabrication have been made as per following fig.3.34 to 3.37.

3.6 Drawing development :

The determined dimension provides the information for drawing development. Assembly and parts drawings are made using Autocad software for outer copper sleeve with graphite fixture and alumina disc. Drawing for inner and outer vacuum leak test sealing arrangement have been also developed. All drawing layouts are shown in fig. 3.34 to fig. 3.37 .

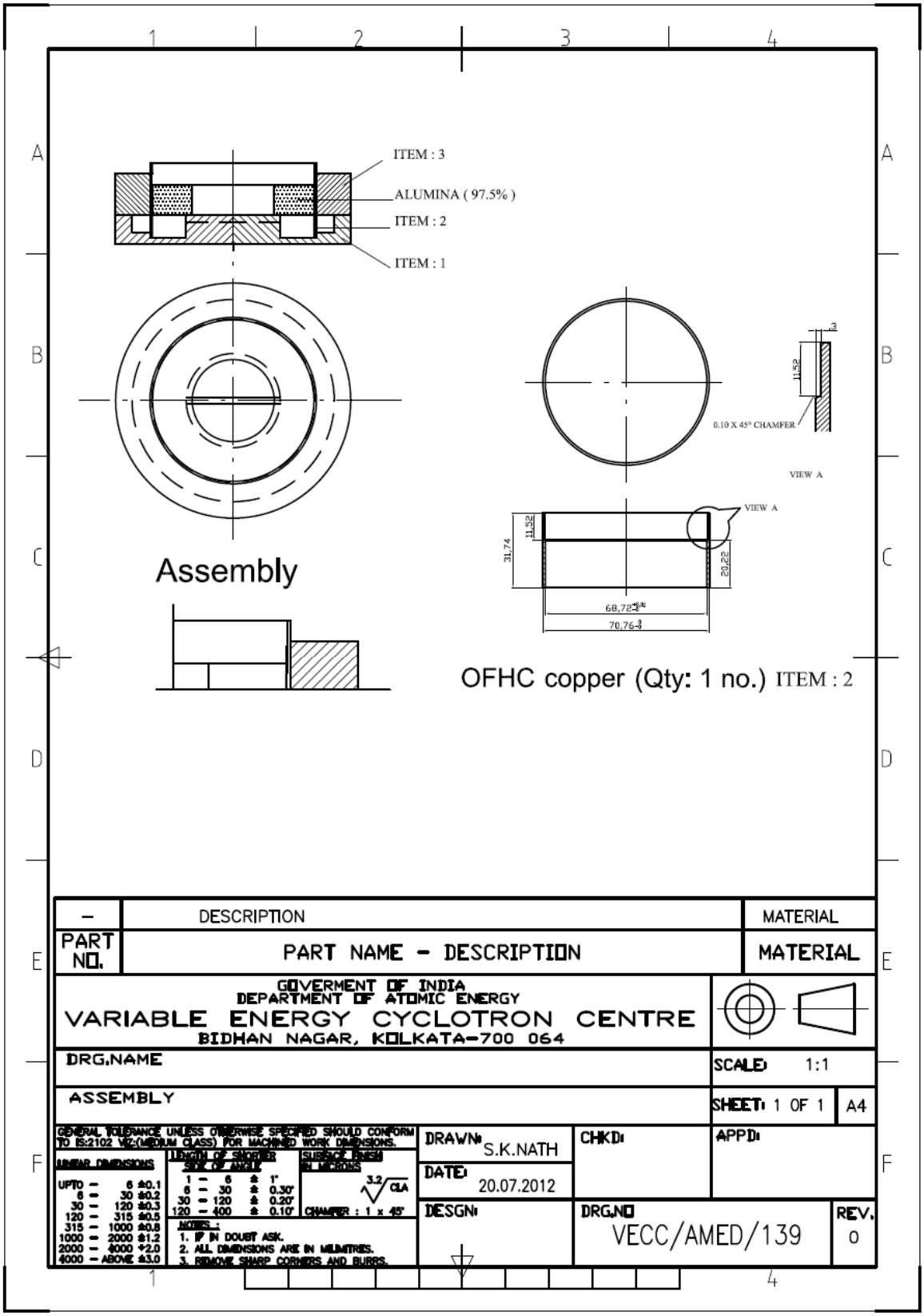

Fig.3.34: Picture of drg. General arrangement of test model with graphite tooling fixture

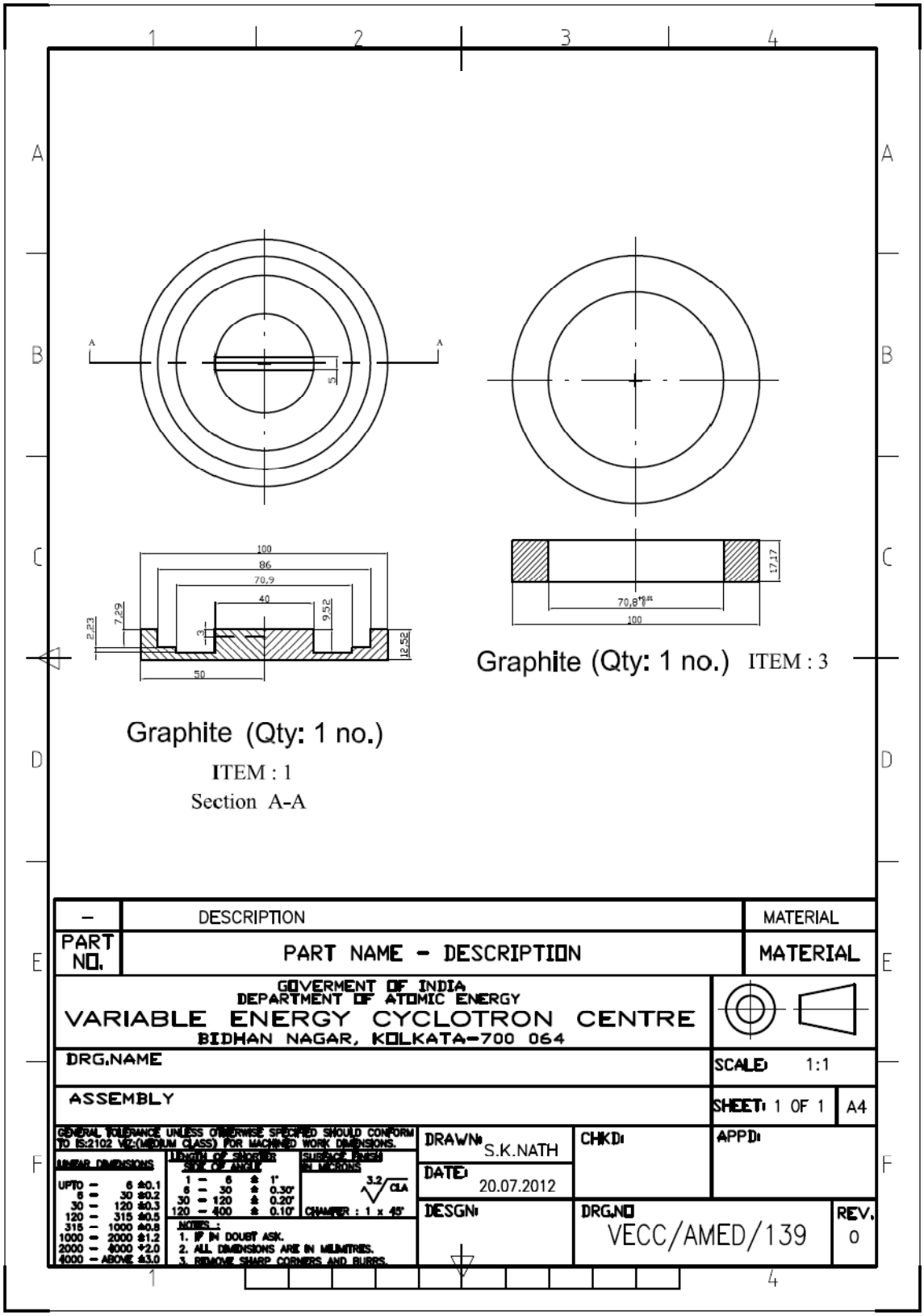

Fig.3.35: Picture of drg. for graphite tooling fixture parts

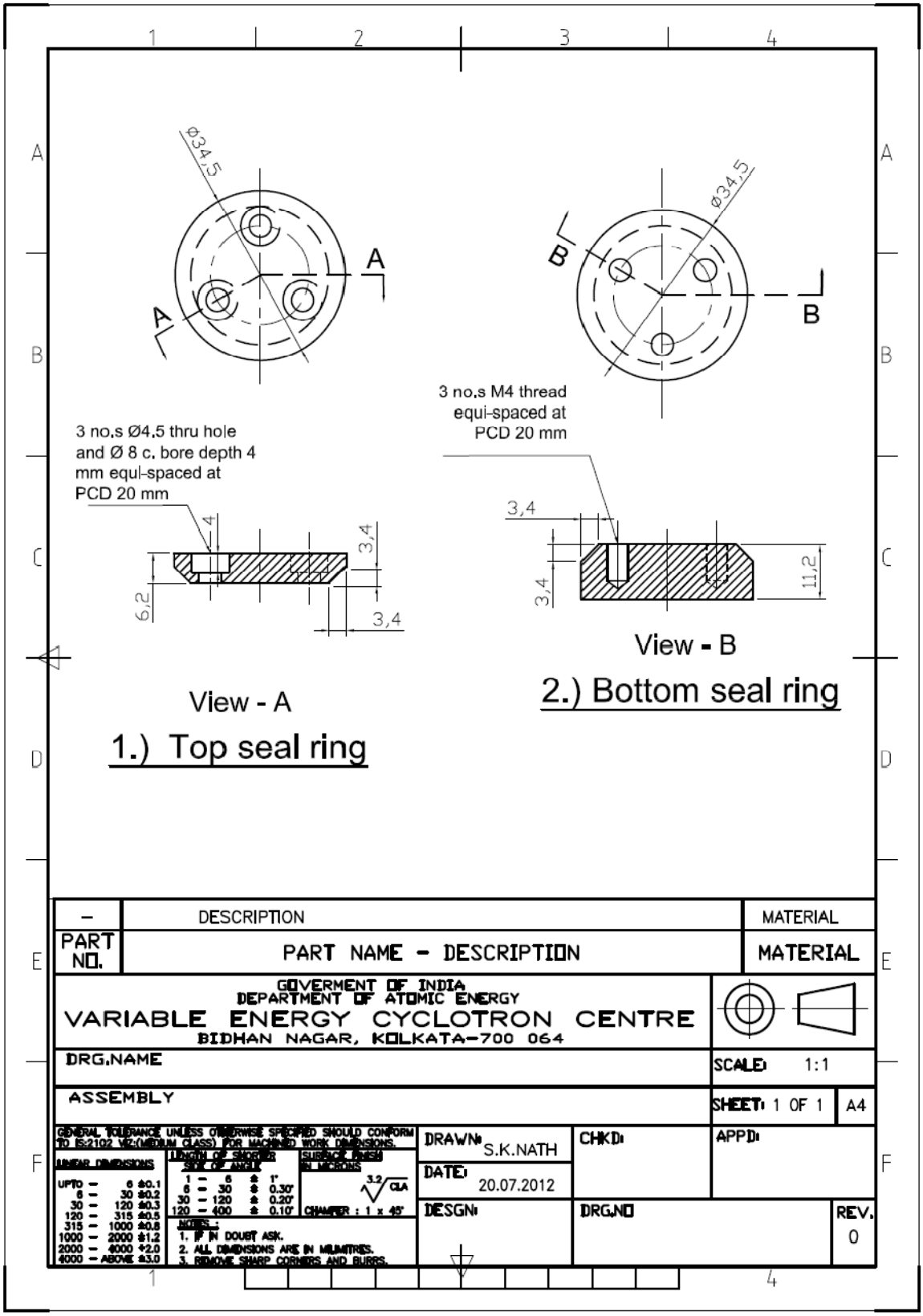

Fig.3.36: Picture of drg. for helium leak detection inside sealing arrangement

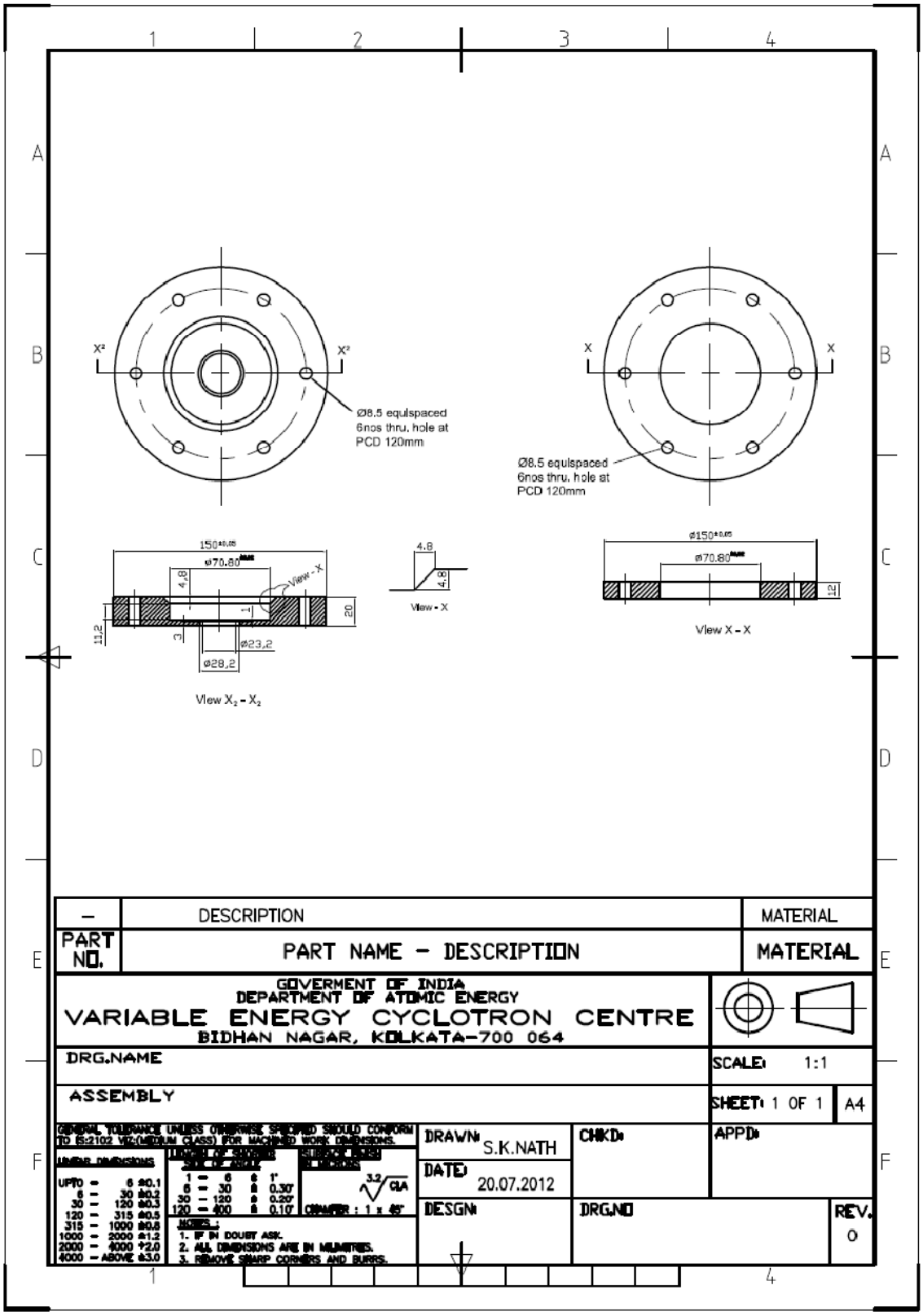

Fig.3.37: Picture of drg. For helium leak detection outside sealing arrangement

Chapter 4

FABRICATION & VACUUM BRAZING PROCESS

4.1 INTRODUCTION

[32, 14] Brazing technique has been used since long for joining metals. Even in today's manufacturing industry, where many operations are carried out automatically using machines, brazing, both mechanized and automated, continues to be an indispensable technique.

The American Welding Society defines brazing as " a group of welding process" which produces coalescence of materials by heating to suitable temperature and using filler metal having a liquidus above 450 ^{0}C and below solidus of the base metal. The filler metal is distributed between the closely fitting surfaces of the joint by capillary action. For brazing to occur, the following three criteria must be met:

- Parts must be joined without melting the base metal
- Brazing filler metal (BFM) must have a liquidus temperature above 450 ^{0}C
- The BFM must wet the base metal surfaces and be drawn into the joint by capillary action

To achieve a good joint using any brazing process the following criteria must be satisfied:

1. The part must be properly cleaned prior to brazing.
2. The part must be protected, either by fluxing or atmosphere during heating process to prevent oxidation
3. The parts must be designed to allow filler metal in molten firm to fill the gap by capillary action

4.2 Need of vacuum furnace brazing

Vacuum brazing is usually a high temperature (typically 927 ^{0}C to 1232 ^{0}C), flux less process using nickel-base, pure copper and less frequently precious BFM. There are several advantages to brazing under vacuum conditions:

- The purity level of the atmosphere (vacuum) can be precisely controlled. Atmospheres of much higher purity can be achieved than can be obtained in regular atmosphere, by reducing the oxygen to less contaminate the work piece.
- The vacuum condition at high temperature results in a decomposed oxides layer, and by doing so improves the base metal wetting properties. Improved wetting will result in better joint properties i.e. increased strength, minimum porosity, etc.)
- Reduced to a minimum distortion because all parts are heated and cooled uniformly at precisely controlled heating/cooling rates
- Repeatability and reliability of the brazing process in modern vacuum furnaces, ideally suitable for complex joint

4.3 Types of vacuum brazing furnace

There are two types of vacuum furnaces available in the industry depending on material used for construction of hot zone. The choice of hot zone construction (heating elements and insulation) depends upon the vacuum level requirement, compatibility with base material and braze filler metals, temperature requirements, and cooling speed. The most suitable choices are graphite and molybdenum.

4.4 Braze Joint Design

4.4.1 Clearance For Vacuum Furnace Brazing

Clearance is the distance between the surfaces of the joint at brazing temperature. Brazed joint clearance has a significant effect on mechanical properties of the joint. For silver, gold , copper and nickel braze filler metals suitable for vacuum brazing, the clearance should be 0.05mm to 0.150 mm . Vacuum brazing requires lower clearance the atmospheric type brazing to obtain optimum strength in the joint. Clearance must be considered at brazing temperature. Between similar metals clearance is easily maintained

in assemblies. With dissimilar metals, the optimum gap clearance of BFM is always specified at brazing temperature.

4.4.2 Effect of Surface Roughness on Braze joint properties

Extensive testing over the years the best surface for brazing is the as –received surface roughness of material coming into the shop. This has received surface may be 32 RMS to 125 RMS. Surface roughness adds surface area to the joint, which provides extra capillary path for filler metal.

4.4.3 Inspection of Test piece components with CMM facility at VECC :

In the present research work all parts of test model have been machined in-house at VECC workshop. Since all parts required very precise tolerance in order of 10 micron. So, parts have been machined, using CNC lathe for copper sleeve and conventional lathe for graphite machining. Alumina ceramic used in this research work is coated with Mo, Mn layer and Nickel plated is ready one from outside vendor. All parts dimensional accuracy has been checked by using CMM and data have been recorded. All parts dimensions were checked and results are found within limit as per drawing and design analysis.

The Inspection of parts is carried out as follows:

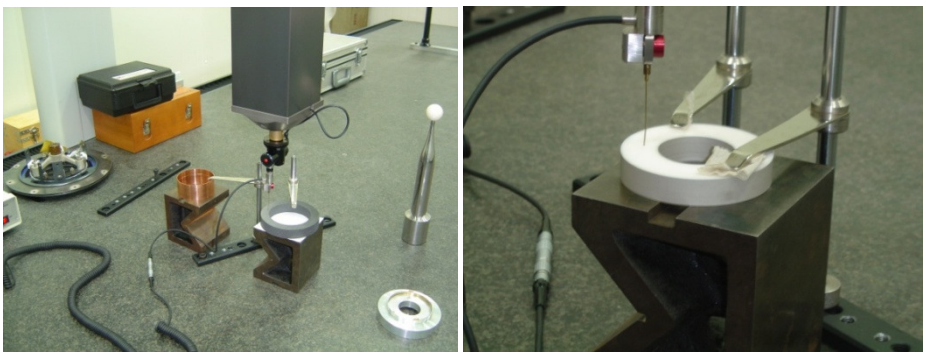

Fig.4.1a, b: Inspection of test sample components with CMM at VECC workshop

Fig.4.1c: Inspection of test sample components with CMM at VECC workshop

4.4.4 Cleaning Procedure prior to vacuum Brazing

Clean, oxide free surfaces are causing to ensure sound brazed joints of uniform quality. Uniform capillary action may be obtained only when all grease, oil, dirt and oxides have been removed from both filler metal and base metal before brazing. Chemical and mechanical cleaning methods are using depending upon various factors. The choice of cleaning process depends on the following:

- Nature of contamination
- Specific base metal to be cleaned
- Degree of cleanliness required for brazing

In the present research work machined parts cleaned by adopting standard pre cleaning process of vacuum brazing. This process involves cleaning of copper part by using acid cleaning, LCW water boiling followed by ultrasonic cleaning using acetone. The steps followed for pre cleanings are as follows:

4.4.5 Pre Cleaning procedure :

Vacuum brazing parts (copper), needs a systematic cleaning procedure to remove foreign particles prior to brazing. The following procedure has been used to clean the part.

1. Degreased with heated trichloroethane with ultrasound bath.
2. Ultrasonic cleaned in alkaline detergent solution 80^{o} C for 5 to 10 minutes
3. Chemical pickling with 10 percent dilute hydrochloride solution in demineralised water for 10 minutes.
4. Immediate rinse with pressurised tap water
5. Rinsing with demineralised water at 80 ^{o}C.
6. Rinsing with acetone
7. Air dries at 80 ^{o}C.
8. Wrapped in aluminum foil and then enclosed in polythene bag.
9. Precaution and corrective measures have been taken for checking pH and resistivity of demineralised water (5 MΩ) and alkaline solution used for cleaning.

Fig.4.2: Machined Copper piece from VECC workshop

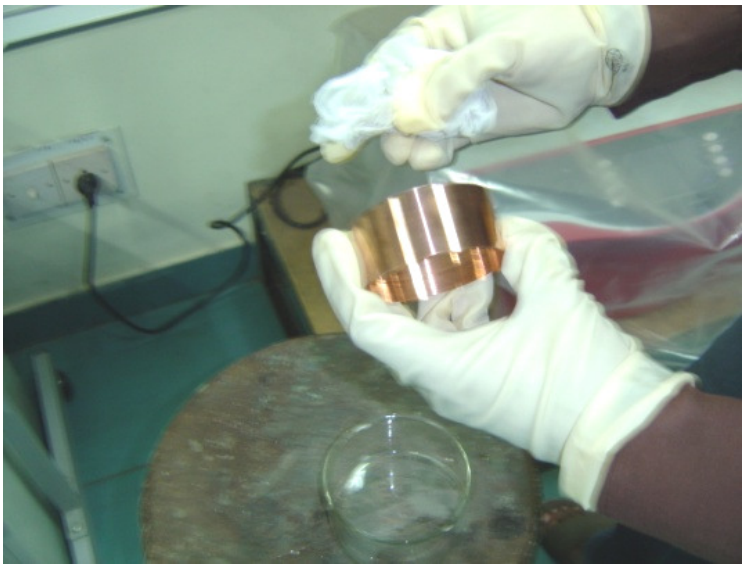

Fig.4.3: Pre-cleaning of copper by chemical pickling

Fig.4.4a, b: Ultrasonic cleaning in acetone

Fig.4.5: Air drying after rinsing with acetone

Fig.4.6: Pre-cleaned copper component

4.5 Vacuum Furnace Brazing Cycles

A properly designed vacuum brazing cycle is a very critical step in the vacuum brazing process. The brazing cycle comprises following segments.

- **Initial pump down**
- **Initial Heating Ramp**
- **Stabilizing Soak**
- **Heating Ramp to Brazing Temperature**
- **Brazing Temperature Soak**
- **Cooling from Brazing temperature**
- **Unloading the Furnace**

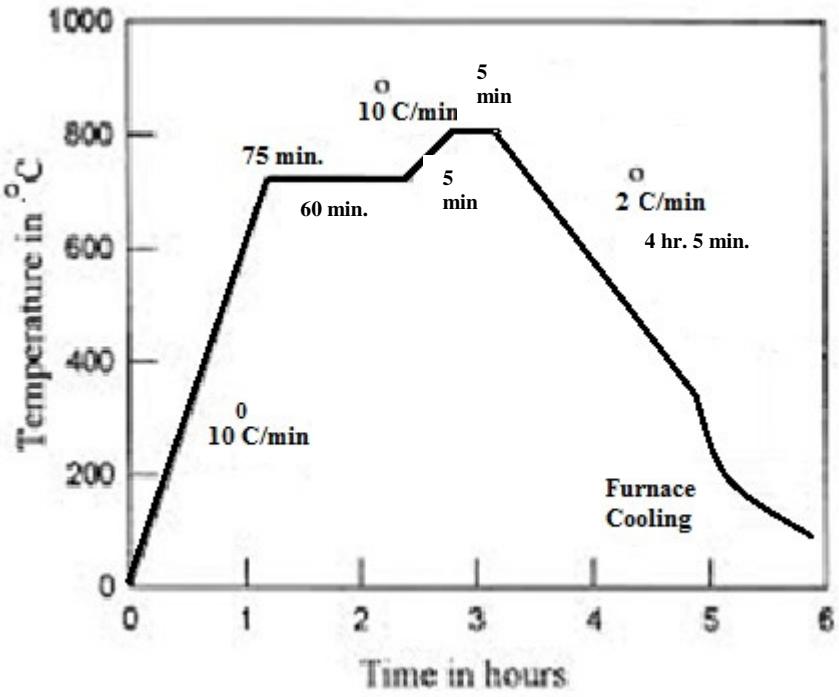

Fig.4.7: Vacuum furnace brazing cycle

a. **Initial pump down :** For easy to braze evacuating vacuum to 8 x 10-4 torr is sufficient; however, for difficult to braze material

b. **Initial Heating Ramp :** The initial ramp should be 10 ^{0} C per min. Faster rates are not recommended because:

- Part distortion may occur
- Brazing slurry application may spill off
- With large loads (containing appreciable amount of brazing slurry) excessive out gassing will likely occur

c. **Stabilizing Soak :** A Soak temperature shall be about 50 ^{0} C below solidus temperature of the brazing slurry for duration of 15 to 30 minutes , or until the pressure drops below the desired level , whichever is longer . In the present research work it was kept 60 min. due to ceramic temperature equalization. This soak serves two purposes :

- It allows the temperature throughout the load to equalize so all parts in the load will reach brazing temperature at approximately the same time during the next heating cycle.
- It ensures that vacuum pressure levels are low enough before proceeding (ramping) to brazing temperature.

d. **Heating Ramp to Brazing temperature:** The final heating rate to brazing temperature is very critical. The rate must be fast enough in normal brazing case in order of 25^{0} C/min, but in present analysis due to alumina ceramic heating rate limitation about 10^{0} C/min has been opted.

e. **Brazing Temperature:** It is desirable to use the lowest brazing temperature within the recommended brazing range. In the present research work eutectic filler Cusil is used. Its solidus and liquidus temperature is same 780^{0}C. But some higher level temperature about 800^{0}C set as brazing temperature to stabilize the temperature in the entire work piece.

f. **Brazing Soak:** In general, time at brazing temperature should be enough to ensure that all parts of work piece reach the desired brazing temperature.

g. **Cooling From Brazing Temperature:** In the present research work cooling rate is very much affect the quality of brazing joint. In this case due ceramic to metal joint the rate of cooling should be very low in order of 2^0 C/min to avoid any crack in the joint or ceramic piece. This cooling rate was maintained from brazing temperature (800^0C) to 300^0C controlled by temperature controller of brazing furnace system. Later on heater was put off and natural cooling takes place about the same order of cooling rate room temperature.

h. **Unloading the furnace:** Brazed assembly can be unloaded when they are at room temperature to avoid any discoloration. The present research test model was unloaded from furnace after 24 hour.[15]

4.6 R.F window outer joint test piece brazing process:

Vacuum brazing test piece was supposed to perform in thermal engineering department NIT Rourkela. It is equipped with PID controlled vacuum brazing furnace. At the starting of research work test piece was kept inside the furnace and vacuum pump started and achieved in order of 3.7 X 10^{-6} mbar. Due to some interlock malfunctions and lack of raw material for re-fabrication of test model and fixture to get fabricated, it was decide to conduct the rest part of work at CGCRI Kolkata. The vacuum brazing furnace at CGCRI is fully automatic controlled supplied by M/s Hindustan high vacuum was tested for complete cycle performs before starting actual brazing. Complete heating, soaking and cooling cycle has been programmed in PID temperature controller. Heating rate has been kept average 10 deg C/Min and cooling rate approx 2 degree per min.

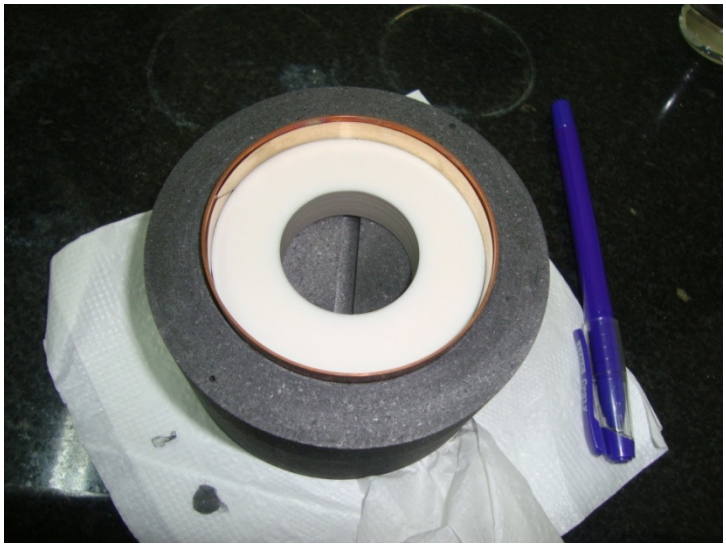

Fig.4.8: Test model assembly (alumina ceramic to metal (Cu) brazing with cusil filler and constrained with Graphite tooling fixture

4.7 Vacuum Brazing Facility at NIT Rourkela:

Vacuum brazing process needs a vacuum chamber in order of 1X10-5 mbar and auto controlled heating elements. At NIT Rourkela vacuum furnace is supplied from srinitech CGCRI having Hind high vac furnace. Details of furnaces are described as follows.

Fig.4.9a: Vacuum brazing furnace at NIT Rourkela

Fig.4.9b: Vacuum level inside the brazing furnace at NIT Rourkela

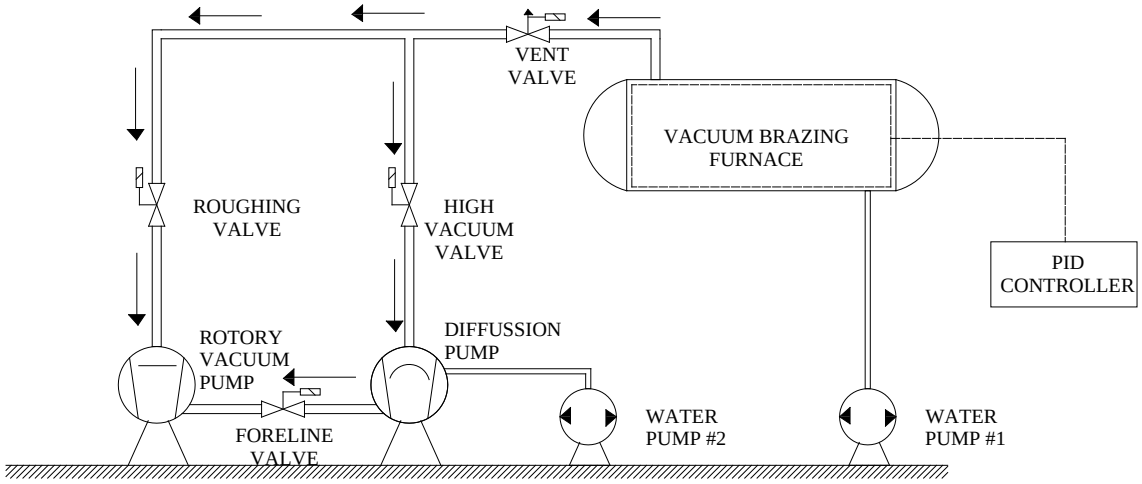

Fig.4.10: Vacuum brazing furnace schematic diagram

4.7.1 Technical Specification of vacuum brazing furnace at NIT:

- **Type:** Horizontal, Cylindrical shaped, water jacketed, front loading type
- **Make:** Srinitech Services, No. 109, Vijay Industrial Estate, Chincholi Bunder, Link Mumbai-400064, Maharashtra, India
- **Function:** Brazing and diffusion bonding of suitable metals

- **Normal operating temperature:** 900^0C (settable) with temperature uniformity of $\pm 5^0$C in space and time
- **Maximum operating temperature:** 1000^0C for one hour
- **Vacuum system: Manually controlled type with:**
    - **a.** Rotary vacuum pump: 15 – 18 m^3/hr
    - **b.** Diffusion pump: 500 L/s (min)
- **Vacuum Level:**
    - **a.** 10^{-5} mbar in cold condition
    - **b.** 10^{-4} mbar in hot condition
- **Hot zone:**
    - **a.** Single hot zone of size: 200X200X500 mm
    - **b.** Temperature uniformity : $\pm 5^0$C
- **Electrical Heating system: Thyristor controlled rectifier type**
    - **a.** Input Voltage : 415 10%, 3 Ph, 4 Wire, 50Hz AC
    - **b.** Input Current : 34 A per phase
    - **c.** DC power output: 15 Kw
- **Modes of operation:**
    - **a.** CVCC mode manual
    - **b.** Temperature control mode (Auto)
- **Cooling water circuit with centrifugal pump and pressure gauge**
- **Temperature measurement:**
    - **a.** Work thermocouple : 2 no's
    - **b.** Over temperature Thermocouple: 1 no.

4.8 Vacuum Brazing Facility at CGCRI Kolkata:

Fig.4.11: Vacuum brazing furnace at CGCRI Kolkata

Central Glass and Ceramic Research Institute (CGCRI) is a set up under the Council of Scientific & Industrial Research at Kolkata. It is one of the renowned R&D organization in the field of ceramic & glass research field. Bioceramics & coating is a division equipped with latest heat treatment & brazing facility. Horizontal Vacuum furnace, Supplied by M/s Hind Havoc India is in the good condition. The present research work brazing part was performed at this institute.

4.8.1 CGCRI Horizontal Vacuum Furnace specifications:

- **Type:** Horizontal, Cylindrical shaped, water jacketed, front loading type
- **Make:** M/s Hind Havoc
- **Function:** Brazing of suitable metals
- **Vacuum:** 5 x 10^{-6} mbar
- **Temp. :** 1400^{0} C (Max.)

- **Hot zone:**

  c. Single hot zone of size: 4 inch. X 4 inch. X 5 inch

  d. Temperature uniformity : $\pm 5^0$C

- Heating element & atmosphere: Molybdenum, Ar, N_2, $H^{2\ atm}$ (optional)

4.8.2 Vacuum brazing process at CGCRI Kolkata:

Fig.4.12: Vacuum brazing test model assembly in hot zone of brazing furnace at CGCRI Kolkata

Fig.4.13: Brazing temperature & vacuum level inside hot zone of brazing furnace at CGCRI, Kolkata

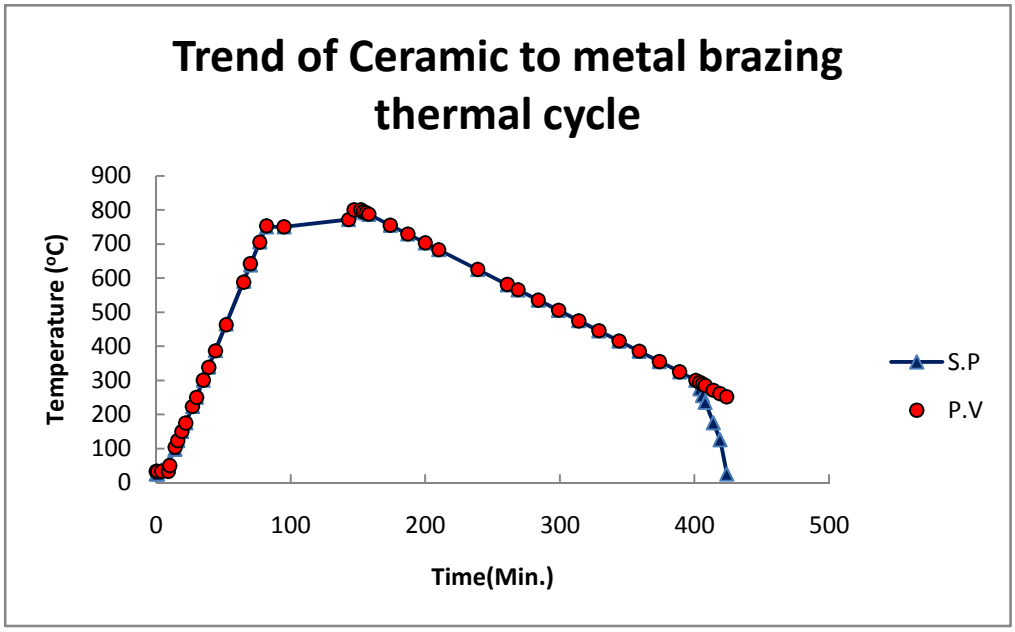

Fig.4.14: Plot of Set value and Process value during brazing cycle (data noted from temperature controller) of vacuum furnace at CGCRI, Kolkata

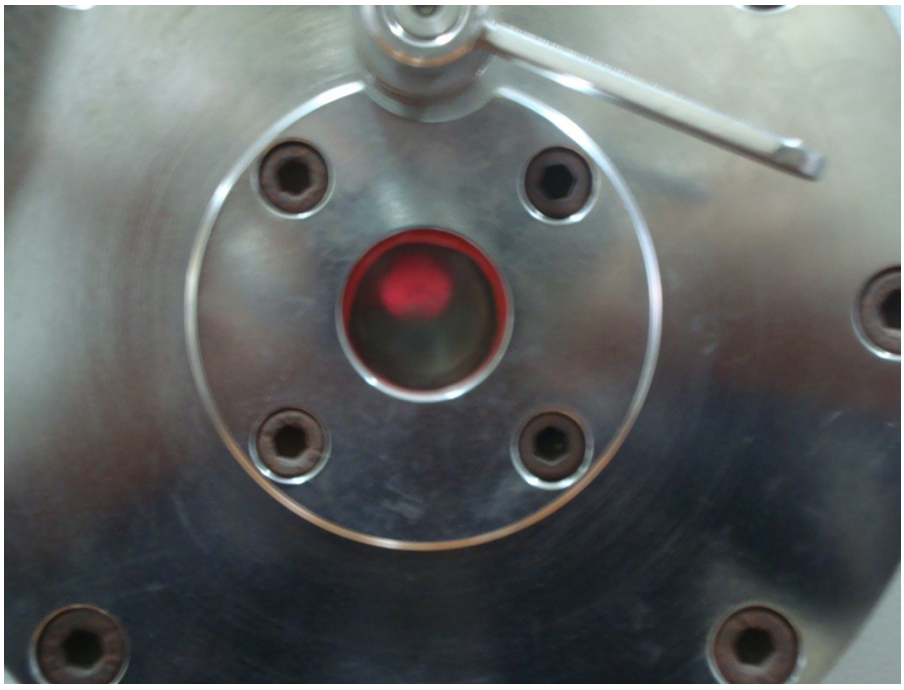

Fig.4.15: Peep hole view of test model inside hot zone at brazing temperature

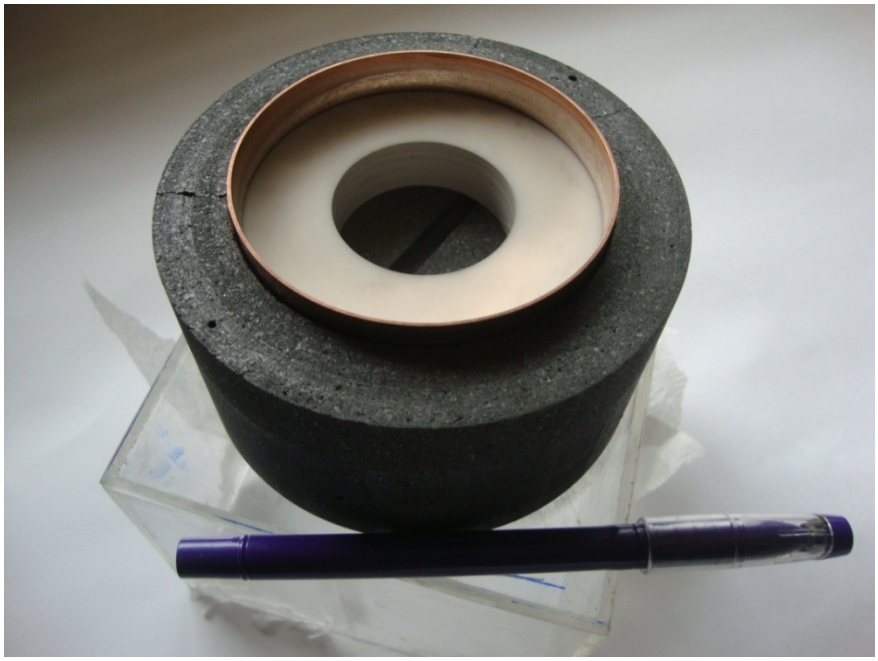

Fig.4.16: Furnace unloaded brazed assembly components

Fig.4.17: Alumina ceramic to metal (Cu) brazed outer joint assembly

Chapter 5

EVALUATION AND QUALITY TEST OF BRAZED JOINT

5.1 INTRODUCTION

The Inspection of the brazed assembly is basically the last step in the manufacturing process. However, quality issues must be addressed at every stage, that is, during the design, prototype development, production, and service of the brazed assembly. [16]

Various NDT inspection methods for brazed joints are defined as follows:

- Visual inspection is the most widely used nondestructive method
  - Limited to external only, no internal imperfections can be revealed
- Leak testing is most advantageous where gas or imperfections can be revealed
  - Limited to low pressure applications
  - Does not assure continued integrity of joint during actual service life of component.
- Vacuum testing has its greatest application where assemblies are to be used in low temperature or vacuum service
  - Limitation requires mass spectrometer and vacuum source
- Proof testing applies a onetime loading that tries to simulate conditions encountered in the service life of brazed components
  - Limitation being it usually cannot simulate all the conditions encountered in the service
  - May not accurately predict service life, especially if cyclic loading occurs

- Radiography is used extensively for brazing joint examination
  - Limitation—many brazed joints cannot be radio-graphically inspected
  - Sensitivities better than 2% are difficult to achieve
  - Special techniques required to reliably inspect joints of varying thickness
  - Multiple views and careful inter interpretation may be required
  - Shows presence of filler material in joint but does not show if a metallurgical bond between base and filler metal is present
- Ultrasonic inspection techniques have been developed and are used for wide range of brazing applications and often are one of the best methods of evaluating joint quality.
  - Limitation being necessary to use a reference standard identical to part being inspected
  - Requires trained operators
  - Method is sensitive to set up variables, part configuration and materials
- Dye and Fluorescent Penetrant Inspection are used for machined surfaces only to detect imperfections open to the surface in both magnetic and non magnetic materials
  - Limited to machined surface only
  - Cannot be reliably utilized on brazed fillets
  - Makes braze repair often difficult or impossible because penetrant and developer cannot be adequately removed
- Thermal transfer inspection is useful in certain specific cases
  - Limited to careful verification of the specific inspection technique to ascertain its acceptance, or lack of, for critical components [17]

5.2 HELIUM LEAK TESTS :

The joints were tested by helium leak detection method. This test has been performed at VECC vacuum section. The test setup has been fabricated and machined at VECC. Details are as follows:

Fig.5.1: Helium leak detection fixture components

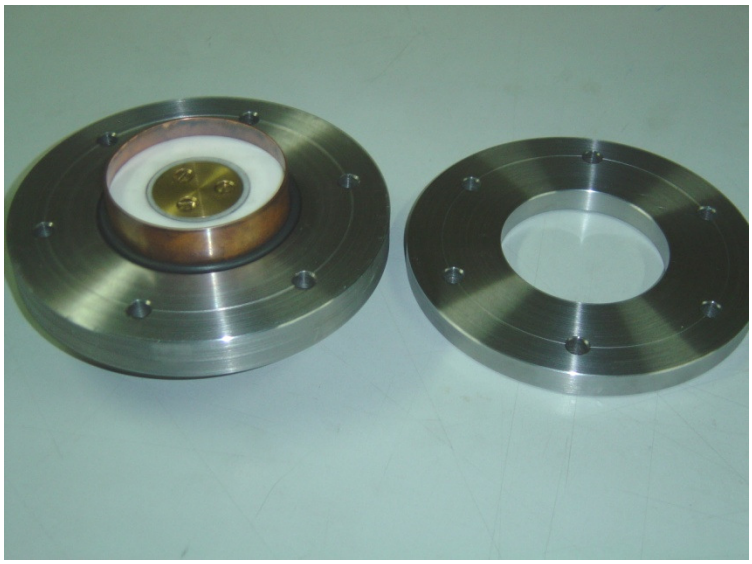

Fig.5.2: Part assembly of ceramic to metal brazed joint leak detection fixture

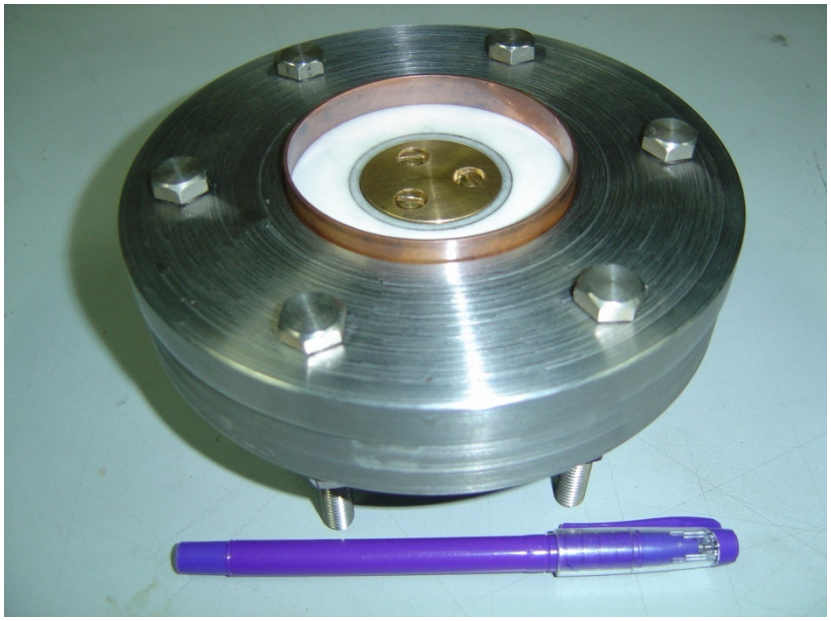

Fig.5.3a: Top View of assembled fixture with test piece for helium leak detection

Fig.5.3b: Front View of assembled fixture with test piece for helium leak detection

Fig.5.4a: Progress of helium leak detection by MSLD method at VECC

Fig.5.4b: Progress of helium leak detection by MSLD method at VECC

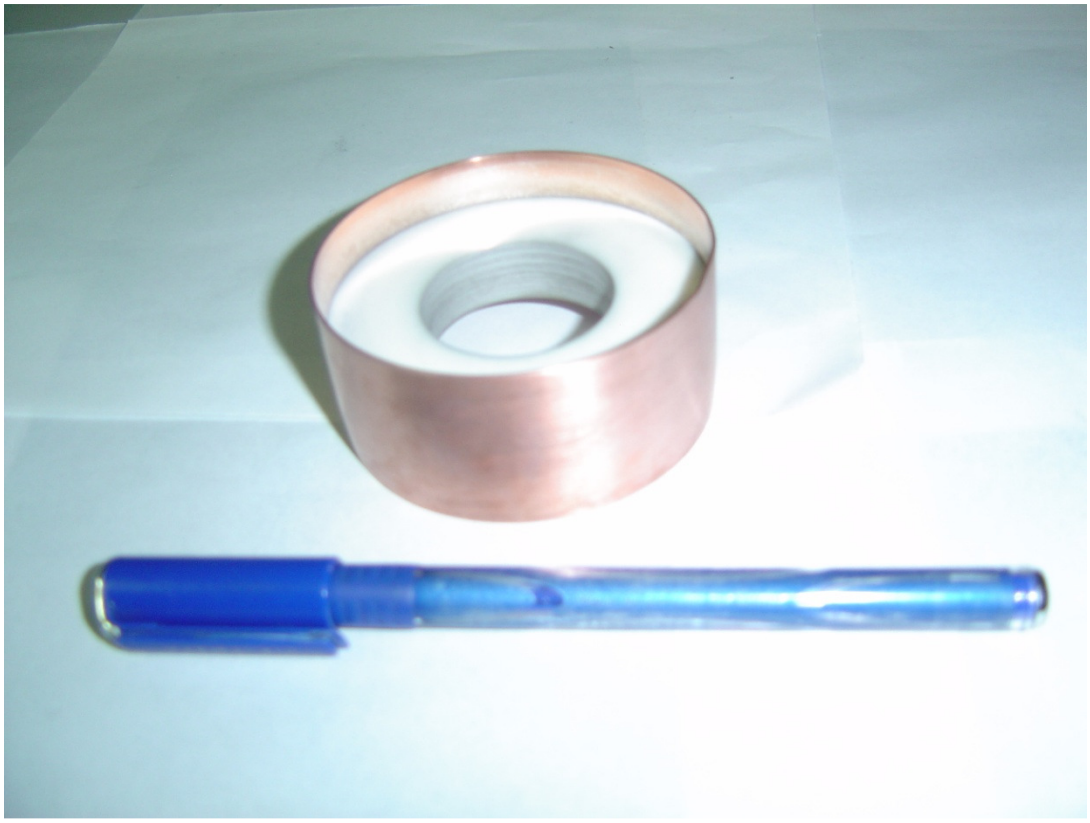

Fig.5.5: Inspected brazed joint assembly

5.3 Result :

The leak test has been conducted and the leak rate found in order of 3.6X10-9 mbar. l/s. The report was recorded and has been produced in next page.

VARIABLE ENERGY CYCLOTRON CENTRE
1/AF,BIDHAN NAGAR , KOLKATA -700 064

Vacuum Section

Ref:- VECC/Vacuum/MSLD/12/10 Date:-27/12/12

Helium leak test report of
Ceramic to metal vacuum brazing of outer joint for R.F.Window Test Model

Date of testing : 27/12/12 , 11.00 Hrs.

Description of the job	:	Ceramic to metal vacuum brazing of outer joint for R.F.Window Test Model
Instrument used for testing	:	Mass Spectrometer Helium Leak Detector, Make : ADIXEN , FRANCE, Model: ASM 142
Smallest detectable signal	:	$5X10^{-12}$ m bar.l/s (He)
Helium Calibrated Leak value	:	$1.2 X 10^{-7}$ m bar l./s
Method of testing	:	Vacuum method (Helium sprayed locally)

Leak detector signal:

Background signal	:	$8.6 X 10^{-10}$ m bar l./s
Final signal	:	$3.6 X 10^{-9}$ m bar l./s

Inspected by :-

27/12/12

Shri Srimanta Bhattacharya, SO/E
Vacuum Section, VECC

Chapter-6

SUMMARY AND CONCLUSIONS

The research reported in this thesis broadly consists of two parts:

- The first part has provided the description of the simulation of ceramic to copper brazing design. It also described the designed dimension comparison through various approach of analysis like analytical, FEM code. Theory of ceramic to metal joining, various joint inspection method requirements as per international standard has also been reported in this part of the thesis. The elasto-plastic simulation has also been reported

- The second part has reported the experimental procedure of ceramic to copper vacuum brazing. It has also reported the pre-cleaning technique and evaluation of joint quality test by helium leak detection method. The drawing developed based on the design data.

6.1 Summary of the Research Findings

The present work has reported the analytical approach supported by FEM technique to simulate the R.F window ceramic to metal joint. A simple model considered to find the proper brazing gap at brazing temperature. It was found that due to different material required to joined (copper outside and alumina inside co-axially placed), the brazing gap at brazing temperature was more than the required for capillary action. To get the proper gap some lower thermal coefficient material is required to prevent the expansion of copper. Molybdenum and graphite both have been considered as the suitable material to serve this purpose subsequently. The simulation reports that in the case of molybdenum as tooling fixture, the gap is achieved at brazing temperature approx. 150 micron whereas its room temperature gap considered 120 micron. In the case of graphite as tooling fixture the brazing gap is achieved approx. 150 micron whereas room temperature gap is required to be kept at 20 micron. This difference was due to

very low thermal coefficient of expansion of graphite. The filler (Cusil) in the form of foil of 0.1 mm thickness used to join the ceramic with copper. It is required to place the filler at the top of the joint by keeping 0.1X3 mm foil at top of joint, so that after melting at brazing temperature it fills the capillary gap. All parts (except alumina ceramic) were machined and finally inspected by using CMM. Pre-cleaning of copper was performed as per standard. All cleaned parts assembled and brazed in vacuum furnace. Evaluation of brazed joint of ceramic to copper outer joint quality test was performed by using helium leak detection method. The result have been found $3X10^{-9}$ mbar L/sec leak rate.

6.2 Conclusions

This analytical and experimental investigation on simulation of ceramic to copper vacuum brazing has led to the following specific conclusions:

1. Successful simulation of ceramic to metal vacuum brazing of R.F window test model for inner and outer joint is possible using proper thermal cycle.

2. This joint was developed by using graphite as tooling fixture material. Graphite is easily available material. The tooling fixture grade of graphite like pyrolitic graphite used to perform this job. Molybdenum is best choice as tooling fixture material because of its low coefficient of thermal expansion, good thermal conductivity and non-hygroscopic property.

3. Evaluation of joint integrity test is required to qualify the mechanical, thermal and electrical RF test. The metallographic test of the joint is needed to enhance the joint integrity. The simulation of inner and outer joint required to simulated for real mode.

4. A number of test piece models are required to be brazed by using molybdenum and graphite separately as tooling fixture with intention to record and analyze of the theoretical and experimental data for technology development. Predictive model based on elasto-plastic analysis approach is successfully applied in this investigation. To predict and simulate the suitable

gap at brazing temperature and find the residual stress after slow cooling testing conditions thus prove a remarkable capability of well-trained ceramic to metal vacuum brazing for modeling concern.

6.3 Recommendations for potential applications

The ceramic to metal vacuum brazing test joint fabricated and experimented upon in this investigation are found to have adequate potential for a wide variety of applications particularly in electrical feed through. Application in airborne electronics for the aerospace - civilian and military, defense devices, medical and analytical instruments, This joint can be used in high-energy physics, high and very high vacuum system ,the nuclear industry etc.

6.4 Scope for future work

This work leaves a wide scope for future investigators to explore many other aspects of such complex joining of ceramic to metal. Some recommendations for future research include:

- Study on the response of these joints to other metal to metal, metal to ceramic or glass.
- Exploration of new fillers like active brazing filler for brazing of non-coated (Mo, Mn) alumina ceramic etc. brazing for development of such hermetic seal.
- Evaluation of brazing joint quality test by thermal, electrical (RF) and mechanical (strength) tests for complete RF window assembly.

References

1. C.W Johnson , “Manual of metal to ceramic sealing technique,” Electronic tube division, sperry Gyroscope company, division of sprerry and corporation great neck, Newyork, by engineering dept.

2. FARRELL L. dEIBEL ,”Calculating residual manufacturing stresses in braze joint using ANSYS”, IEEE Transaction on electron devices. Vol. ED-34, No. 5, May 1987

3. R.A Rimmer, “A high power L band RF window”,2001, Particle accelerator conference, Chicago

4. Michal Neubaur, “Rugged ceramic window for RF application”, PAC09

5. M.Neubaur, “High power RF window and coupler development for PEP II B Factory”, SLAC, Pub-95-6897

6. M.Neubaur, “High power coax window”, IPAC10, Kyoto Japan

7. Jkokavec and L Cesnak , “Mechanical stress in cylindrical superconducting coil”, J.Phys. D:Appl. Phys,Vol. 10, 1977

8. T Nowak, “Analytical and numerical study on thermally induced residual stress in multilayer cylinder”, 9th International congress on thermal stress, June 5-9,2011, Budapest

9. E.Chin and E.E Reis, “Elastic-Plastic-creep analysis of brazed carbon-carbon/OFHC Divertor Tile concept for TPX”, IEEE 95

10. Panayiotic J Karditsas and Marc- Baptiste, “ Thermal and structural properties of fusion related materials” , UKAEA FUS 294, June 1995

11. JanuSz Kowalewski and Jansusz szczurek, “ Heat treating progress”, May/June 2006

12. M. Samandi, “ Application to ceramic / metal joining, Nuclear instruments and method in physics research , 1997

13. A K Jadoon, “Metal to ceramic joining via a metallic interlayer bonding”, Journal of material processing technology , 2004

14. Janusz Kowalewski, “ Issues in vacuum brazing”, Seco/Warwick, Meadville, PA USA, heat treating progress, June 2006

15. Kay D. Brazing fundamental- “ Differential metal Expansion”

16. Sulzer Metco – Introduction to Brazing (2004)

17. M.Ahmmed#, A. Dutta Gupta, Theoretical analysis and fabrication of coupling Capacitor for k500 superconducting cyclotron at Kolkata. Variable Energy Cyclotron Centre, Kolkata, published in Proceedings of CYCLOTRONS 2010, Lanzhou, China

18. ZHANG Yong, “Progress in joining ceramics to metal”, journal of iron and steel research, international, 2006, 13(2):01-05

19. O. Kozlova, Brazing copper to alumina using reactive CuAgTi alloys ,Elsevier, 19 Oct 2009

20. Cazajus V, “ Thermal stresses in ceramic-metal composite after brazing process”, ICSAM 2005

21. P.Zaccaria, “ Thermal-mechanical analysis of large ceramic rings during brazing process, Elsevier, 29 may 2007

22. Toru Kishii, “ Method of Thermal stress calculation for circular cylinder and disc:, Journal of ceramic society of Japan, 21 may 1993

23. Gyorgy SZABO, “ thermal strain during czochralski growth”, journal of crystal growth, 6 June 1985

24. M.R Eslami, “ Thermal and mechanical stresses in a functionally graded thick sphere”, international journal of pressure vessel and piping, Jan 17, 2005

25. Peaslee R.L. “ The Brazement-Design and Application” ASM Publication Paper Number 61-WA-2589

26. W.D Kingery, " Factor affecting thermal stress resistance of ceramic materials", Journal of The American ceramic society-Kingery, Vol. 38 No. 1

27. Ramesh kumar, " Mechanical design and fabrication of input coupler and sensing loop coupler for Indus-I rf cavity

28. S. Bini, " X-Band RF structure thermal analysis and tests", nuclear Instruments and method in physics, may 14 2007

29. H. Ghasemi, " Alumina copper eutectic bond strength: Contribution of preoxidation, cuprous oxides particles and pore", Mechanical engineering, Vol. 16, No. 3, pp. 263-268.Sharif university of technology, June 2009

30. Kar A, Mandal S, Venkateswarlu K, Ray AK, Characterization of interface of Al2o3-304 stainless steel braze joint, Material characterization, volume 58, Issue 6, June 2007, pages-555-562

31. Ajoy K. Ray, Abhijit Kar, "Graphite-to-304SS Braze joining by active metal-Brazing technique: Improvement of mechanical properties", Journal of materials engineering and performance, April 25, 2012

32. Yuji Kato, " Recent developments in vacuum brazing furnace technology", ULVAC TECHNICAL JOURNAL (English) No. 71 E 2009

33. "Fundamental of Brazing" Seminar by Key & Associates, Phoenix AZ, May 2005

34. "ANSYS user manual"

35. M.H Sloboda "Design and strength of braze joint", , Johnson Matthey & Co. Ltd London

36. " Umicore AG & Co. KG "Design of brazed joint

37. "American welding society – Brazing" Handbook, fourth edition (1991)

38. M.Schwartz " Brazing for the engineering technologist"

39. John F.Harvey, P.E "Theory and design of pressure vessels"

40. S.P Timoshenko and J.N Goodier "Theory of elasticity, Third edition"

41. A. Kandil, a.a el-kady and A.El –kafrawy, “Transient thermal stress analysis of thick-walled cylinders”, by Production engineering department, Faculty of engineering in port said, suez canal university port said Egypt, int J. Mech. Sci, vol 37, pp 721-732

42. Naotake Node, Richard B. hetnarski, Yoshinobu Tanigawa, “Thermal stresses” ASTM. Annual book of ASTM standard, vol. 10.04: 25. West Conshocken, PA: ASTM; 1996

43. S Timoshenko Strength of material, Part I and II

44. P K Nag, “ Engineering Thermodynamics”

45. “S.P Timoshenko and J N goodier” Theory of elasticity

46. Erdogan Madenci and Ibrahim Guven, “The finite element method and Application in engineering using ANSYS “

47. IS standard, UDC 669.28-422.2

48. L.S Srinath, “ Advanced mechanics of solids third edition”, Tata McGraw-Hill ,2011,

49. www.matweb.com,

50. www.sciencedirect.com,

51. www.wikipedia.org,

52. www.ferp.ucsd.edu/LIB/PROPS,

53. www.wesgometal.com,

54. www.nist.org,

55. www.espimetals.com,

56. www.ceramics.nist.gov,

57. www.molybdenumpowder.com,

58. www.morgantechnicalceramics.com,

59. www.kxcad.net,

60. www.wisetool.com,

61. www.edfagan.com,

62. www.azom.com,

63. www.vacaero.com

Publication

Conference

[1] S. Singh[1], M. Ahammed[1], T.K. Bhattacharyya[1], B. Hembram[1], A. Dutta Gupta[1], G. Pal[1] and A. Chakrabarty[1], **"**Design and fabrication of the cryoshocking test facility for in-house development of 4K-2K cryo-insert", NSC-24, IPR Ahmedabad ,Jan 21-24 2013

APPENDIX

Annexure-1

1. Thermo-mechanical properties of material

1.1. AVERAGE MATERIAL PROPERTIES

MATERIAL PROPERTY, BOUNDARY CONDITION, LOAD						
Property	Density	Modulus of Elasticity	Thermal expansion (20^0C)	Thermal conductivity (Average)	Specific heat capacity (Average)	Poisson ratio
Value in metric unit	Kg/m^3	GPa	$^0C^{-1}$	W/(m*K)	J/(Kg*K)	
OFHC (99.95%) REF[53]	8.94×10^3	117	19.13×10^{-6}	487.22	439.89	0.31
Alumina (97.5 %), REF[57]	3.97×10^3	331	7.89×10^{-6}	8.524	1202.22	0.231
CuSil Ag- 72%,Cu-28%, REF[54]	10×10^3	830	19.6×10^{-6}	371	385	0.36
Molybdenum 99.5%, REF[62]	10.24×10^3	330	5.4×10^{-6}	110.22	301	0.38
Graphite,REF[53]	2.21×10^3	6	1.6×10^{-6}	686	1632	0.31
Boundary condition	Uy=0					
Thermal load	Temperature (Steady state), Tref = 300K, Tbraz = 1100K					

Table 8.1: Average properties of materials

1.2. TEMPERATURE DEPENDENT MATERIAL PROPERTIES

TEMPERATURE DEPENDENT MATERIAL PROPERTIES OF Copper, Molybdenum, and Graphite											
SL.No.	Materials using in analysis	Thermo-mechanical Properties	Unit	Temperature (K)							
				293	473	673	873	923	1023	1100	1200
1	OFHC Copper (Cu.), Ref[9]	Modulus of Elasticity	GPa	96.6	91.8	82.8	69	65.5	57.3	57.3	57.3
		Thermal expansion	$\mu m/m\ ^0C^{-1}$	16.8	17.4	18.1	18.8	19	19.7	19.7	19.7
		Poisson ratio		0.33	0.33	0.33	0.33	0.33	0.33	0.33	0.33
2	Molybdenum-num (Mo.), Ref.[53]	Modulus of Elasticity	GPa	330	323.47	311.84	306.61	301.68	297	292.4	283.64
		Thermal expansion	$\mu m/m\ ^0C^{-1}$	5.08	5.12	5.23	5.29	5.37	5.45	5.53	5.73
		Poisson ratio		0.356	0.356	0.356	0.356	0.356	0.356	0.356	0.356
3	Alumina (Al- 97.5%.), Ref.[53]	Modulus of Elasticity	GPa	385.169	372.348	357.696	343.044			326.352	319.012
		Thermal expansion	$\mu m/m\ ^0C^{-1}$		0.114	0.267	0.424			0.609	0.7
		Poisson ratio									
4	Graphite (C) Ref.[53]	Modulus of Elasticity	GPa	5.34	5.36	5.452	-	5.48	5.59	5.8	6.044
		Thermal expansion	$\mu m/m\ ^0C^{-1}$	0	0.001	0.117	-	0.15	0.201	0.28	0.392
		Poisson ratio		0.14	0.14	0.14	-	0.14	0.14	0.14	0.14
TEMPERATURE DEPENDENT MATERIAL PROPERTIES OF Cusil filler											
5	Cusil Filler, Ref. [2]	Thermo-mechanical Properties	Unit	Temperature (^0C)							
				25	200	400	600	800	1000	1100	-
		Thermal expansion	$\mu m/m\ ^0C^{-1}$	14.3	16.6	17.2	18	19.8	22.6	22.6	

Table 8.2: Temperature dependent properties of material

Annexure-2

2. Model Governing Equation

2.1 Equation for Temperature distribution :

Considering a long coaxial cylinder of two materials, with material 1 in the region a≤ r ≤ b and material 2 in the zone b≤ r ≤ c. The heat transfers of both materials use the following governing equation

$$\kappa_i\left(\frac{\partial^2 T_i}{\partial r^2}+\frac{1}{r}\frac{\partial T_i}{\partial r}\right)=\frac{\partial T_i}{\partial t}, \tag{2.1}$$

in which the subscript i means material (i = 1, 2) and T, κ, r and t are the temperature, thermal diffusivity, radius and time, respectively. Assume that initially the temperature inside the structure is zero and the boundary conditions are

$$T_1(a,t)=T_2(a,t),\ -\kappa_1\frac{\partial T_1(a,t)}{\partial r}=-\kappa_2\frac{\partial T_2(a,t)}{\partial r},\ -\kappa_2\frac{\partial T_2(b,t)}{\partial r}=\varepsilon\sigma T^4 \qquad \text{(2.2a-c)}$$

2.2 Equation for Thermal stress distribution :

In order to calculate the thermal stress distribution in thick wall cylinder under the assumption made in chapter 3, (3.1), The following lami's equation obtained from equilibrium equation considered,

$$\frac{d\sigma_r}{dr}+\frac{\sigma_r-\sigma_\theta}{r}=0 \tag{2.2.1}$$

Thermal stress produces due to temperature distribution in material or due to different material having different linear coefficient of expansion are in contact. Our case is second one in which following approach has been used. Where σ_r and σ_θ are the radial and hoop stress, respectively.

The general stress-strain-temperature relation can be written as followings:

$$\begin{aligned}
\varepsilon_r &= \frac{1}{E}\left(\sigma_r - \nu\left(\sigma_\theta + \sigma_z\right)\right) + \alpha\Delta T_0 \\
\varepsilon_\theta &= \frac{1}{E}\left(\sigma_\theta - \nu\left(\sigma_z + \sigma_r\right)\right) + \alpha\Delta T_0 \\
\varepsilon_z &= \frac{1}{E}\left(\sigma_z - \nu\left(\sigma_r + \sigma_\theta\right)\right) + \alpha\Delta T_0
\end{aligned} \tag{2.2.2}$$

Where E and ν are the Young modulus and Poisson ratio, respectively and α denotes a thermal expansion coefficient. The equivalent temperature change, ΔT_0 contributes to the residual stresses developed during brazing process and dependent upon the brazing temperature.

Assuming now that plane sections remain plane, i.e. the longitudinal (axial) strain is constant across the wall of the cylinder. The hoop and radial strain in eq. (2.2.2) can be expressed by the r-direction displacement, u_r as :

$$\varepsilon_\theta = \frac{u_r}{r}, \qquad \varepsilon_r = \frac{\partial u_r}{\partial r}, \qquad \varepsilon_z = const, \tag{2.2.3}$$

It can be easily proved , that equation (2.2.1) is solved by:

$$\begin{cases} \sigma_r = C_1 - \dfrac{C_2}{r^2} \\ \sigma_\theta = C_1 + \dfrac{C_2}{r^2} \end{cases} \tag{2.2.4}$$

where C_1 and C_2 are constants, which can always be find out if any pressure conditions like $-p_a$ and $-p_b$ are defined.

After substituting equation (2.2.2) & (2.2.4) into equation (2.2.1), displacement u_r

can be calculated as following:

$$u_r = \frac{1}{E(b^2 - a^2)}\left[(1-\nu)\left(a^2 p_a - b^2 p_b\right)r + (1+\nu)a^2 b^2 \left(p_a - p_b\right)\frac{1}{r}\right], \qquad (2.2.5)$$

In case of temperature load of compound cylinder of different material (low thermal expansion coefficient material as out-side & high thermal expansion coefficient material as inside tube of compound cylinder), there can be some interface stresses p_b generated between the layers, depending on the differences in thermal expansion coefficients of the materials. To find out the stress-strain field within the compound cylinders we must calculate interface pressure p_b first.

The interface at radius r=b is an algebraic sum of the radial displacement of outer inside layer and inner outside layers:

$$\delta_b = b\left[\frac{-k_1}{E_1} p_a \left\{\frac{1}{E_1}\left(k_2 - \nu_1\right) + \frac{1}{E_2}\left(k_3 + \nu_2\right)\right\} p_b - \frac{k_4}{E_2} p_a\right] \qquad (2.2.6)$$

where E_1 , E_2 and ν_1 , ν_2 are the Young modulus and Poisson ratio of inner and outer cylinder respectively, and :

$$k_1 = \frac{2a^2}{b^2 - a^2}, \qquad k2 = \frac{a^2 + b^2}{b^2 - a^2}, \qquad (2.2.7a\text{-}2.2.7d)$$

$$k_3 = \frac{b^2 + c^2}{c^2 - b^2}, \qquad k_4 = \frac{2c^2}{c^2 - b^2},$$

The interface displacement δ_b due to change in temperature ΔT can be defined by following expression:

$$\delta_b = b\Delta T\left(\alpha_1 - \alpha_2\right), \qquad (2.2.8)$$

Assuming the external pressure zero, the interface pressure can be calculated as

followings :

$$p_b = \frac{\Delta T.(\alpha_1 - \alpha_2)}{\frac{k_3 + \nu_2}{E_2} + \frac{k_2 - \nu_1}{E1}}, \tag{2.2.9}$$

Radial & Hoop stress for Cylinder under external pressure

$$\sigma_{r(Cu.)} = \frac{-b^2.p_b}{b^2 - a^2} + \frac{p_b.a^2.b^2}{b^2 - a^2}.\frac{1}{r_{Cu.}^{\ 2}} \tag{2.2.10}$$

$$\sigma_{\theta(Cu.)} = \frac{-b^2.p_b}{b^2 - a^2} - \frac{p_b.a^2.b^2}{b^2 - a^2}.\frac{1}{r_{Cu.}^{\ 2}} \tag{2.2.11}$$

General displacement equation for Cylinder under internal & external pressure

$$u_{r(Cu.)} = \frac{1}{E_1.(b^2 - a^2)}\left[(1-\nu_1).\left(a^2.p_a - b^2.p_b\right)r_{Cu.} + (1+\nu_1).a^2.b^2\left(p_a - p_b\right).\frac{1}{r_{Cu.}}\right] \tag{2.2.12}$$

Radial & Hoop stress for Cylinder under internal pressure

$$\sigma_{r(Mo.)} = \frac{-b^2.p_b}{c^2 - b^2} - \frac{p_b.a^2.b^2}{c^2 - b^2}.\frac{1}{r_{Mo.}^{\ 2}} \tag{2.2.13}$$

$$\sigma_{\theta(Mo.)} = \frac{-b^2.p_b}{c^2 - b^2} + \frac{p_b.a^2.b^2}{c^2 - b^2}.\frac{1}{r_{Mo.}^{\ 2}} \tag{2.2.14}$$

General displacement equation for Cylinder under internal & external pressure

$$u_{r(Mo.)} = \frac{1}{E_2.(c^2 - b^2)}\left[(1-\nu_2).\left(b^2.p_b - c^2.p_c\right)r_{Mo.} + (1+\nu_2).b^2.c^2\left(p_b - p_c\right).\frac{1}{r_{Mo.}}\right] \tag{2.2.15}$$

[Ref. (8),(39),(40),(48)]

3. Technical Specification of R.F Window

Operating frequency	:	9 - 27 MHz
Max. Power to be transfer	:	80 kW
Max. Voltage to be supplied	:	100 kV
Permissible helium leak rate	:	$< 1X10^{-8}$ mbar-l/sec
Material of Conductor	:	OFHC copper
Material of ceramic	:	99.97% pure Alumina

General arrangement drawing of the coupling capacitor showed with R.F window has been presented in Fig 1.2 at the beginning of this chapter.